# Investigation of a Suitable Shear Friction Interface between UHPC and Normal Strength Concrete for Bridge Deck Applications

Final Report
May 2017

BRIDGE ENGINEERING CENTER

About the Bridge Engineering Center

The mission of the Bridge Engineering Center (BEC) at Iowa State University is to conduct research on bridge technologies to help bridge designers/owners design, build, and maintain long-lasting bridges.

Technical Report Documentation Page

1. Report No. InTrans Project 10-379	2. Government Accession No.	3. Recipient's Catalog No.
4. Title and Subtitle Investigation of a Suitable Shear Friction Interface between UHPC and Normal Strength Concrete for Bridge Deck Applications		**5. Report Date** May 2017
		6. Performing Organization Code
7. Author(s) Sriram Aaleti (orcid.org 0000-0002-8738-454X) and Sri Sritharan (orcid.org/0000-0001-9941-8156)		**8. Performing Organization Report No.** InTrans Project 10-379
9. Performing Organization Name and Address Civil, Construction, and Environmental Engineering Iowa State University 2711 South Loop Drive, Suite 4700 Ames, IA 50010-8664		**10. Work Unit No. (TRAIS)**
		11. Contract or Grant No.
12. Sponsoring Organization Name and Address Iowa Department of Transportation 800 Lincoln Way Ames, IA 50010	Federal Highway Administration 1200 New Jersey Avenue, SE Washington, DC 20590	**13. Type of Report and Period Covered** Final Report
		14. Sponsoring Agency Code SPR UHPC-011

15. Supplementary Notes

Visit www.intrans.iastate.edu for color pdfs of this and other research reports.

16. Abstract

The current National Bridge Inventory database lists the concrete bridge deck deterioration, in the form of reinforcement corrosion or concrete distress, as one of the leading causes of structural deficiency. The combination of aging infrastructure, growing number of structurally deficient or obsolete bridges, and continuous increase in traffic volume in the United States demands rapid improvements to the nation's bridge infrastructure with an emphasis on increasing bridge longevity. A recent Highways for LIFE project sponsored by the Federal Highway Administration (FHWA) entitled Full Depth UHPC Waffle Bridge Deck Panels confirmed the significant benefits of ultra-high performance concrete (UHPC) deck systems in terms of excellent structural performance, durability, and ease of construction. However, the initial capital cost of this deck system is comparatively higher than the traditional, normal strength concrete decks, which may hinder the wider usage of UHPC waffle decks in bridges. In order to overcome this challenge and to improve longevity of bridge decks, this project explores the possibility of using a thin layer of UHPC overlaying a normal strength concrete (NC) deck.

The behavior of the interface connection will have a significant impact on the overall structural and durability performance of the UHPC-NC composite deck system. Consequently, an integrated experimental and analytical study was conducted at Iowa State University to understand the influence of several variables, such as normal concrete strength, interface roughness, and curing condition on the shear transfer behavior across the interface between UHPC and NC. The laboratory testing was performed in two phases, including slant shear testing in Phase I and flexural testing of composite deck specimens in Phase II. A total of sixty test units with five different surface textures and three different concrete strengths were loaded to failure. Then, five 8 in. thick, 2 ft wide, and 8ft long deck specimens with 1.5 in. thick UHPC overlays were tested to failure. With the interface texture being the main variable, the composite deck sections were subjected to a combined monotonically increasing flexure and shear loading. The slant shear test results demonstrated that the shear transfer across the interface for all five different textures is adequate for overlay applications, which was later confirmed by the composite deck sections tests. Based on the experimental results, the researchers found that the current AASHTO 2010 guidelines provide a conservative estimate for the UHPC-NC interface shear strength.

17. Key Words accelerated bridge construction—bridge deck overlays—bridge deck rehabilitation—precast bridge sections—ultra-high performance concrete		18. Distribution Statement No restrictions.	
19. Security Classification (of this report) Unclassified.	**20. Security Classification (of this page)** Unclassified.	**21. No. of Pages** 80	**22. Price** NA

Form DOT F 1700.7 (8-72)   **Reproduction of completed page authorized**

INVESTIGATION OF A SUITABLE SHEAR FRICTION INTERFACE BETWEEN UHPC AND NORMAL STRENGTH CONCRETE FOR BRIDGE DECK APPLICATIONS

Final Report
May 2017

Principal Investigator
Sri Sritharan, Professor
Civil, Construction, and Environmental Engineering, Iowa State University

Research Assistant
Sriram Aaleti, Assistant Professor
Civil, Construction, and Environmental Engineering, University of Alabama

Authors
Sriram Aaleti and Sri Sritharan

TABLE OF CONTENTS

LIST OF FIGURES

LIST OF TABLES

ACKNOWLEDGMENTS

1   INTRODUCTION

1.1 Background

According to the National Bridge Inventory, the average age of bridges in the United States is 43 years. A large percentage of the bridges in the United States will be reaching their intended design service life of 50 years in the coming decade. Also, more than 10.4% of bridges in the United States are listed as structurally deficient, while over 13% are rated as functionally obsolete (Transportation for America 2013). Bridge decks are particularly vulnerable to a wide selection of damages resulting from freeze-thaw cycles, exposure to deicing salts, and deterioration as a result of dynamic loads from vehicular traffic and plow trucks. Cracking in bridge decks is a common problem in the United States, and the deterioration of bridge decks is a leading cause for bridges receiving obsolete or deficient inspection ratings (ZellComp, Inc. 2011, Stanfill-McMcillan and Hatfield 1994). The exposure of bridge deck steel to a combination of high moisture, varying temperatures, and corrosive chlorides from de-icing salts through surface cracks leads to concrete deterioration and loss of serviceability. These in turn lead to bridge deck replacement or major repairs (see Figure 1).

Figure 1. Deteriorated bridge decks across several states in the United States

Overlays are often applied to bridge decks to extend the life of the bridge by providing protection from water and chemical penetration and by creating a durable wearing surface. The overlay also has to provide adequate bearing capacity that is compatible with the loading of the bridge deck. These characteristics will be fulfilled when the overlay concrete achieves an optimal strength and a resistance to crack propagation.

According to the Federal Highway Administration (FHWA), $200 to $300 billion dollars is needed to rehabilitate or replace all structurally deficient bridges in the nation. The combination of an aging infrastructure, a growing number of structurally deficient or obsolete bridges, and a continuous increase in traffic volume in the United States demands rapid improvements to the nation's bridge infrastructure with an emphasis on increasing bridge longevity. Hence, federal, state, and municipal bridge engineers are seeking alternative ways to build better bridges, reduce travel disruptions, and improve repair techniques, thereby reducing maintenance costs and increasing bridge longevity. Additionally, owners are challenged with replacing critical bridge components, particularly bridge decks, during limited or overnight road closure periods. Consequently, there is a growing need to develop technologies that are not only economical and durable but can also be safely and rapidly implemented in practice.

1.2 Scope of Research

Ultra-high performance concrete (UHPC) is a self-leveling high-strength concrete material with excellent durability (Graybeal 2006a) and tensile strength (Sritharan et al. 2003) when compared to normal strength concrete (NC) used in today's bridge construction. This unique combination of properties makes UHPC an ideal material for minimizing deck cracking and associated bridge deterioration. Consequently, UHPC has gained significant momentum in terms of its utilization in bridge applications among several departments of transportation (DOTs) and the FHWA. A recent project entitled Full Depth UHPC Waffle Bridge Deck Panels confirmed the significant benefits of UHPC deck systems in terms of excellent structural performance and ease of construction (Aaleti et al. 2011). However, the initial capital cost of a UHPC bridge deck is comparatively higher than the traditional normal strength concrete deck, which may hinder the wider usage of UHPC decks in bridges.

The researchers wanted to find a way to minimize the cost of a UHPC deck system while realizing the benefits of UHPC in decreasing the deck deterioration that occurs due to the formation of cracks as well as the penetration of deicing chemicals placed on the top surface. As a possible solution, they developed a composite bridge deck concept by overlaying a thin UHPC layer onto a NC slab. To facilitate the application of the concept in both new and existing bridge decks, no mechanical connection between the UHPC and NC was considered appropriate. This composite deck system not only provides a cost-effective solution by reducing the amount of UHPC by up to 50% in comparison to the waffle deck system but also yields a highly durable alternative to the traditional concrete deck system, which has high maintenance costs.

However, a performance characterization of the composite deck system is essential to make this concept a reality for field applications. As illustrated in previous successful rehabilitation projects (Denarié 2005), the behavior of the interface connection plays a significant role in the overall structural and durability performance of the UHPC-NC composite deck system. However, the shear friction characteristics of the UHPC and NC interface and the factors influencing its behavior are largely unknown and need investigation in order to make this composite deck a reasonable solution for bridge applications. This research investigates the feasibility of using UHPC as a thin-bonded overlay on concrete bridge decks or developing a precast UHPC-NC composite deck system with UHPC topping for new decks.

1.3 Report Organization

The second chapter of this report is a review of the literature describing previous experimental and analytical studies performed in order to understand the interface behavior between concretes poured at different times. This chapter also summarizes the recent experimental studies examining the performance of UHPC and normal concrete behavior in the United States. Chapter 3 discusses the experimental testing of composite specimens that was performed as part of this research. The details about fabrication, testing methods, and results are also presented in this chapter. The conclusions from this study along with recommendations for field implementation are presented in the final chapter.

2   LITERATURE REVIEW

2.1   Bridge Rehabilitation using Overlays

Current National Bridge Inventory databases list concrete bridge deck deterioration, in the form of reinforcement corrosion or concrete distress, as one of the leading causes of structural deficiency in bridges. The distress to the concrete can result from freeze-thaw damage, abrasion damage, alkali-aggregate reactivity, excessive cracking, and/or spalling caused by corrosion of the reinforcement. Throughout the United States, DOTs are concerned about the maintenance and rehabilitation of bridge decks. With the limited availability of funds and the time needed for bridge deck replacement, transportation agencies are eager to extend the service life of existing bridge decks with effective rehabilitation methods.

Although bridge design guidelines published by the DOTs often specify mix designs and construction methods in their efforts to minimize concrete bridge deck deterioration, bridges needing deck habilitation continue to be a major maintenance challenge. Bridge deck rehabilitation methods vary widely throughout the United States. The main objective for choosing any rehabilitation technique, including choosing a specific rehabilitation material, is to provide the already distressed deck concrete and reinforcement adequate protection from the environmental effects that will continue the deterioration process. The main rehabilitation procedures currently used for in-the-field applications include overlays, membranes, sealers, and cathodic protection. When deciding on an appropriate bridge rehabilitation method, state DOTs consider several factors, including bridge rating; traffic volume; bridge condition; traffic delays; and the costs of bridge repair, rehabilitation, or replacement. However, as the frequency of deck deterioration due to deck reinforcement corrosion increases, more attention is given to rehabilitation strategies involving overlays, especially low-slump, dense concrete overlays, and latex modified concrete overlays with increased concrete cover to prevent chlorides from reaching the reinforcement. These strategies have had mixed success in improving the service life of concrete bridge decks.

An overlay creates a protective barrier over a concrete bridge deck to prevent water, oxygen, and especially chlorides found in deicing agents from penetrating the bridge deck. Installation of an overlay is often considered when (1) the deck has little to moderate deterioration but is likely to experience deterioration in the future and so is not in need of immediate replacement or (2) the deck is in a very high traffic area where it would be expensive and disruptive to replace the deck using staged construction. An overlay provides a new wearing surface so that problematic deck surface conditions, such as cross-slope and grade, joint transitions, drainage, abrasion resistance, and skid resistance, along with scaling problems, can be improved. To ensure successful rehabilitation, surface preparation is necessary to provide the required bond between the overlay and the deck. Bonded overlays normally add structural capacity to the deck because they thicken the deck; however, overlays add dead load to the supports and the substructure. The amount of additional dead load is reduced by using thin overlays or by milling the concrete cover (surface preparation) prior to placing the overlay. Usually it is recommended to leave at least 1/2 to 1 in. of original concrete cover over the reinforcing steel bars to maintain bar encapsulation (Krauss et al. 2009).

Overlays can be either single-layered or double-layered. Single-layered overlay systems are homogenous mixtures of chemicals and aggregates, while double-layered overlay systems have two distinct layers: a lower layer that is effective at water proofing and an upper layer that provides skid resistance and protects the lower layer from the damaging effects of traffic. The most commonly used overlays consist of asphalt, latex modified concrete, silica fume concrete, low-slump dense concrete, fly ash concrete, or polymer concrete. National Cooperative Highway Research Program (NCHRP) Synthesis 333 provides information on previous and current designs and construction practices used to improve the performance of deteriorated bridge decks as follows (Russell 2004):

> **Low-Slump Dense Concrete Overlays:** Low-slump dense concrete overlays are produced using a concrete with cement content as high as 800 lb/yd^3 and a water to cementitious material ratio (w/cm) as low as 0.30. These overlays were first used in the 1960s in Iowa and Kansas. Initially, overlays were no more than 1.25 in. thick (Bergren and Brown 1975); however, later a nominal thickness of 2 in. was specified. These types of overlays are commonly used in Iowa even today.

> **Latex Modified Overlays:** Latex modified concrete consists of a conventional Portland cement concrete supplemented by a polymeric latex emulsion. The use of latex modified concrete overlays was previously reported to be more widespread than low-slump concrete overlays; a number of states preferred the system because of its ease of application. However, it was reported that, shortly after placing, numerous cracks were observed (Steele and Judy 1977).

> **Polymer Concrete Overlays:** Polymer concrete is produced by replacing the Portland cement with a polymer. Overlays made with polymer concrete are generally less than 0.5 in. thick. In the 1990s, the Missouri DOT used epoxy–polymer overlays to rehabilitate bridge decks. The overlays consisted of a thin, two-part epoxy with aggregate filler and a minimum 0.25 in. thickness (Kepler et al. 2000). A number of different materials for polymer concrete overlays were investigated in the late 1970s and early 1980s, but most have since been discontinued (Kepler et al. 2000).

Latex modified concrete overlays and low-slump dense concrete overlays have, in general, performed satisfactorily. However, traditional overlays have several limitations. For instance they have relatively short service lives (typically between 5 to 25 years), necessitating continuous maintenance, repair, and replacement of the system. These repetitive installations drain the financial resources of state and national transportation agencies (Krauss et al. 2009). Furthermore, several traditionally used overlays, requiring experienced contractors and/or specialized equipment for correct application, can significantly add to the structure's dead load, and they often have compatibility challenges associated with differences in time-dependent characteristics, especially shrinkage, between the old concrete in the deck and overlay material (Krauss et al. 2009).

UHPC has several unique properties that make it a potentially desirable material for overlay applications. These properties include extremely high permeability resistance, negligible dry

shrinkage when thermally cured, and high post-cracking tensile resistance. The idea of using UHPC as an overlay material primarily comes from its high strength and durability. Normally, UHPC has a compressive strength of about 22 ksi and a tensile strength greater than 1.5 ksi (Sritharan 2015). Additionally, UHPC exhibits extremely low permeability, which largely prevents the ingress of detrimental substances such as water and chloride ions. These characteristics suggest that UHPC could be an attractive alternative to conventional overlay materials when it comes to protecting the concrete material below the overlay. The properties of UHPC potentially allow for a thinner topping than conventional overlaying materials, and its qualities of being self-consolidating and highly moldable allow it to flow easily and bond with the lower surface during installation. If a strong mechanical bond is formed between the two surfaces and a high-quality surface with high abrasion resistance is obtained, the application of UHPC as an overlay could result in significant enhancements that would prolong the service life of a concrete bridge deck.

2.2 Ultra-High Performance Concrete

UHPC is defined worldwide as concrete with a compressive strength of at least 22 ksi (Schmidt and Fehling 2005). In recent years, Lafarge North America has marketed Ductal, a form of UHPC containing steel fibers, which regularly achieves compressive strengths of about 26 ksi. Other UPHC materials are also beginning to surface in the United States market. UHPC is an advanced, highly engineered, cementitious material consisting of typical Portland cement and a fine aggregate made of sand, silica fume, crushed quartz, steel fibers, super plasticizers, and high water reducers. The typical composition of UHPC is shown in Table 1.

Table 1. Material composition of typical UHPC mix

Material	Amount, lb/yd^3	Percent by Weight
Portland Cement	1200	28.5
Fine Sand	1720	40.8
Silica Fume	390	9.3
Ground Quartz	355	8.4
Super plasticizer	51.8	1.2
Accelerator	50.5	1.2
Steel Fibers	263	6.2
Water	184	4.4

Source: Graybeal 2006a

A few notable differences in the composition of UHPC as compared to high performance concrete (HPC) include the lack of coarse aggregate, the addition of steel fibers, a high proportion of cementitious materials, and a low water/cement ratio. The use of powder and well-graded components helps in achieving the high packing density of the UHPC constituents and leads to significantly improved mechanical properties, such as increased compressive strength and considerable tensile strength as compared to HPC and normal strength concrete. In addition, UHPC demonstrates a very dense cement matrix, which results in a low permeability concrete and greatly enhances its resistance to corrosion and degradation. In precast environments, UHPC

is commonly subjected to heat treatment of 194 °F combined with 95% humidity conditions to accelerate the full development of its strength and durability. However, these conditions are not required for curing UHPC. Ambient curing may also be appropriate, depending on the constraints set forth by the specific application. For example, field-cast UHPC connections between precast elements are not typically heat cured. More details about curing conditions and their influence on UHPC material behavior are presented in the material properties section below.

The use of steel fibers in UHPC improves the material's ductility as well as its tension capacity. In addition to the advantages realized from its superior mechanical and durability properties, which result from the use of super plasticizers in the mix design, UHPC also displays self-consolidating/self-leveling behavior, allowing it to be placed in plant and field conditions with little to no vibration, reducing construction placement costs.

The properties of UHPC suggest the potential to improve the overall economy of construction projects significantly. The high compressive strength of UHPC allows designers to select smaller dimensions for members, decreasing dead load on the structure and improving overall structural efficiency. UHPC also displays rapid early strength gain, which, in addition to being suitable for precast/prestressed applications, can contribute to reduced construction time. Finally, the superior durability characteristics of UHPC should contribute to an increased service life and to reduced maintenance costs compared to conventional concrete structures in nearly all applications. Therefore, in the current-day concrete technology, UHPC can arguably be considered an ideal structural material.

2.2.1 Material Properties

This section summarizes the material behavior of UHPC under various loading conditions.

2.2.1.1   Compressive Stress-Strain Behavior

The compressive strength of the building material is one of the critical parameters in the design of concrete structures. The characteristic compressive strength of UHPC is defined in a similar fashion as NC's compressive strength: by its 28-day strength. The applicability of the standard ASTM International's compression testing method to evaluate the compressive behavior of UHPC has been studied by several researchers (Graybeal 2006a, Ahlborn et al. 2008). Based on this research, it was found that a standard ASTM test using a 3 in. $\times$ 6 in. cylinder with appropriate surface preparation and a load rate of 150 psi per second can be utilized for compression testing to determine the characteristic compressive strength of UHPC (Graybeal 2006a).

UHPC has very high compressive strength compared to NC or typical HPC used in current-day practice due to its high-density matrix and its absence of coarse aggregate. Based on the commercially available products in the market today, the characteristic 28-day compressive strength (f_c') for UHPC ranges from 18 to 33 ksi, depending on the type of curing process (Perry

and Zakariasen 2004, Kollmorgen 2004, Graybeal 2006a, Ahlborn et al. 2008). A steam-cure treatment for 48 hours at a temperature of 194°F is typically used to achieve the full compressive strength, especially in precast environments. An FHWA study completed on more than 1,000 compression test samples of UHPC produced by Lafarge North America showed that the average compression strength at 28 days is 18.3, 28, 24.8, and 24.8 ksi for air, steam, delayed steam, and tempered steam curing conditions, respectively (Graybeal 2006a).

A recent study conducted by the Michigan DOT on the same type of UHPC reported compressive strengths of 23.9 ksi and 30.5 ksi for air-cured and steam-cured specimens (Ahlborn et al. 2008). These strengths are higher than those found in previous studies. In addition, it was found that under steam curing conditions the characteristic strength of UHPC was reached after three days of casting (which included two days of steam curing). For air-cured specimens, the UHPC strength gradually increased with time, reaching strengths of 14 ksi and 19 ksi after three days and seven days, respectively. Furthermore, a recent FHWA study investigating the effects of curing temperature on the compression behavior of non-steam-cured UHPC suitable for field-cast applications found that UHPC achieved a compressive strength of 22.5 ksi to 24.5 ksi at 28 days when curing temperatures of 50 °F, 73 °F, and 105 °F were used (Graybeal and Stone 2012). Therefore, the compressive stress-strain behavior of UHPC is well established, based on the summary of the above-mentioned studies and the compressive strength reported in real-world UHPC bridge projects (Bierwagen and Abu-Hawash 2005, Keierleber et al. 2008, Wipf et al. 2009, Rouse et al. 2011, Graybeal 2007). The results of numerous concrete compressive cylinder tests are shown in Figure 2(a). Design behavior is shown in Figure 2(b).
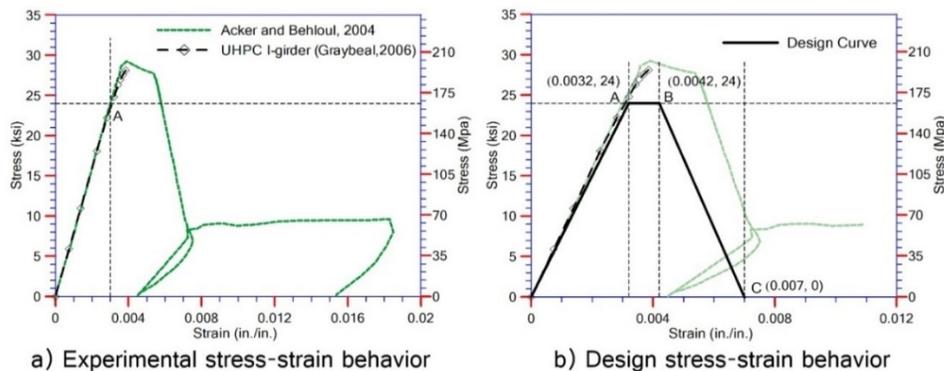
Aaleti et al. 2013

Figure 2. Actual and recommended design stress-strain behavior of UHPC in compression

The same 2006 FHWA study notes that the strain value corresponding to the peak compressive strength is about 0.0035 and 0.0041 for air- and steam-cured specimens, respectively (Graybeal 2006a, Graybeal 2012b). In addition, unlike the stress-strain relationship found in NC, the measured stress-strain relationship for UHPC was found to be linear for levels up to 80 to 90% of the peak stress for both curing conditions (see point A in Figure 2(a)). However, according to Sritharan et al. (2003), heat-treated UHPC exhibited linear elastic behavior up to failure, corresponding to a compressive strain of 0.0032.

2.2.1.2   Tensile Stress-Strain Behavior

The inclusion of steel fibers in the composition of UHPC results in a dependable tension capacity for the material. Consequently, the tension capacity of UHPC can be relied upon at the ultimate limit state when utilizing it in design. This is in contrast to the design of members using normal concrete, where the concrete tension capacity is ignored after cracking. The tensile strength and post-cracking behavior of UHPC depends on the strength, quantity (e.g., volume by percentage), length, and orientation of steel fibers, which effectively prevent or delay the opening of concentrated cracks. The tensile strength is also influenced by the type of curing treatment (steam- or air-cured) provided for UHPC members.

An investigation conducted by the FHWA examined four different methods for evaluating the tensile behavior of UHPC, including the flexural prism test, the split cylinder test, the mortar briquette ("dog-bone") test, and the direct tension test (Graybeal 2006a). Although all four of the test methods provided realistic tensile cracking strengths, the results varied by 0.5 ksi, depending on the test method. Therefore, the study conservatively recommended that the cracking tensile strength of UHPC be taken as 1.3 ksi and 0.9 ksi for steam-cured and untreated (i.e., air-cured) conditions, respectively. As a follow-up to a series of compression and flexural tests (Sritharan et al. 2003), a set of direct tension tests were conducted on large, steam-cured dog-bone specimens, producing tension parameters comparable to those resulting from the FHWA study. The tensile stress-strain behavior established by these dog-bone tests, which have been used successfully in characterizing the flexural response of UHPC full-scale bridge girders, tapered H-shaped piles, and waffle deck panels, is shown in Figure 3(a). Proposed design stress-strain behavior is illustrated in Figure 3(b).

a) Experimental and proposed stress-strain behavior   b) Proposed design stress-strain behavior
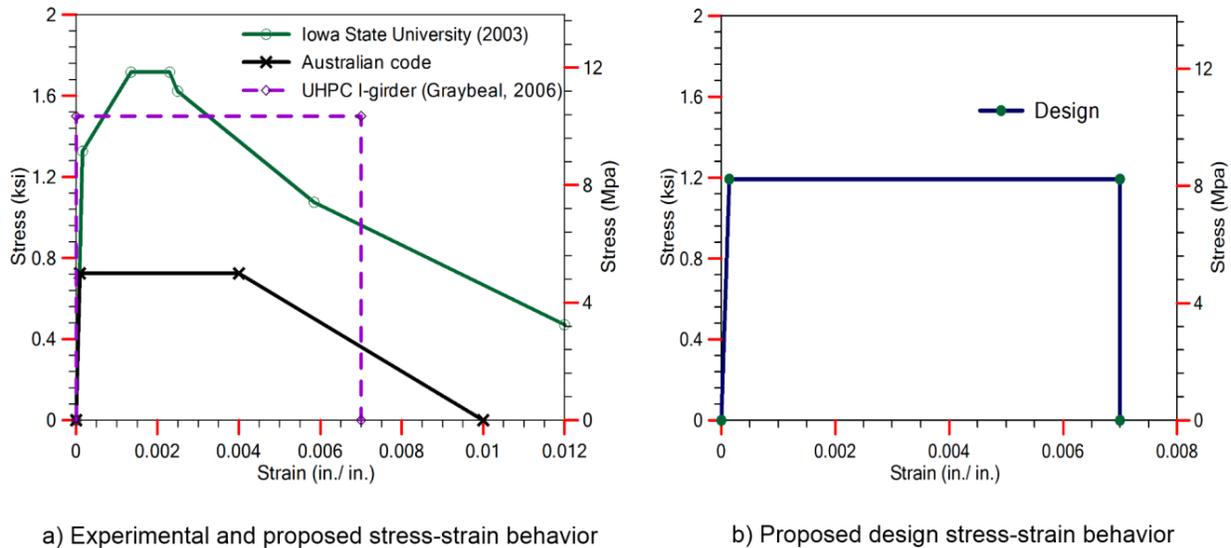
Aaleti et al. 2013, FHWA Highways for LIFE

Figure 3. Measured and recommended design stress-strain behavior of UHPC in tension

Based on the back analysis of large-scale UHPC I-girder tests under flexure and shear, Graybeal (2006b) proposed a conservative approximation of the UHPC tensile stress-strain behavior for use in estimating the ultimate capacity of the UHPC sections. Accordingly, UHPC under tension can be assumed to behave in an elastic-perfectly plastic fashion with a post-cracking capacity of 1.5 ksi for strains below the pullout strain of 0.007 (see Figure 3a).

In a recent study on the tension behavior of UHPC, Graybeal and Baby (2013) used a direct tension test method using dog-bone shaped test specimens of different sizes. These tests characterized the tension behavior of UHPC under different curing conditions and differing steel fiber quantities. This study noted that the tensile response of UHPC consists of the following four phases: elastic behavior, inelastic cracking, straining in discrete cracks, and single crack localization. Results from these tests also confirmed that the tensile response of UHPC can be represented with an elastic-perfectly plastic response for design purposes, as suggested in Figure 3b.

2.2.1.3   Density

The density of UHPC is slightly higher than that of HPC or NC due to its very compact microstructure. The average reported value for the density of UHPC mixes from 17 published mix descriptions was approximately 157 lb/ft^3 (Vande Voort et al. 2008). A unit density of 155 lb/ft^3 was suggested by studies done in the United States (Graybeal 2006a, Ahlborn et al. 2008).

2.2.1.4   Coefficient of Thermal Expansion

UHPC tends to exhibit a higher coefficient of thermal expansion (CTE) than NC. This may be attributed to the fact that UHPC contains a comparatively high volume of cementitious materials (relatively high CTE) without any coarse aggregate, which has low CTE values. The FHWA and Michigan DOT studies recommended a value of about 8.2 x 10^{-6}/°F for CTE (Graybeal 2006a, Ahlborn et al. 2008). The Michigan study found that this value can be used once thermal treatment has been completed, regardless of the age of the concrete. For comparison purposes, the expected CTE for NC is about 6.0 x 10^{-6}/°F and for HPC it is between 4.0 and 7.3 10^{-6}/°F (AASHTO 2010).

2.2.1.5   Shrinkage Behavior

UHPC exhibits relatively significant shrinkage behavior in comparison to normal concrete due to its high cementitious material content; therefore, it is more susceptible to cracking under restrained conditions. A recent study by Graybeal (2006a) found that UHPC exhibited rapidly occurring, large-value, early-age shrinkage strains. The shrinkage strains in heat-treated UHPC were nearly 850 microstrains during the curing period. Untreated UHPC also exhibited shrinkage strains beyond 790 microstrains. Although the shrinkage strain in UHPC is higher than in NC, shrinkage in UHPC takes place early in its life cycle. In fact, heat-treated UHPC does not exhibit any significant shrinkage in the post-treatment period. In the absence of heat treatment, specimens reached 95% of ultimate shrinkage at the age of two months (Graybeal 2006a).

Because UHPC cracks in tension at strains lower than these shrinkage strains (see tensile behavior), it is important to mitigate or eliminate shrinkage restraints in UHPC structural members during casting.

2.2.1.6   Chloride Penetration Resistance

UHPC exhibits very low to negligible permeability when compared to NC due to its high-density matrix and low water/cement ratio. The ASTM C1202 standard, commonly known as the rapid chloride ion penetrability test, can be used to estimate the chloride resistance of UHPC. In the study by Graybeal (2006a), the chloride penetration resistance of specimens receiving any of the four curing regimes at 56 days and those receiving any form of heat treatment at 28 days achieved a negligible rating (< 100 coulombs). Only untreated specimens at 28 days did not receive this rating; those specimens averaged passing 360 coulombs of charge, resulting in a very low permeability qualification. Similarly, Ahlborn et al. (2008) reported negligible chloride penetrability for all specimens tested in their study. Graybeal (2006a) used another test procedure, known as the chloride ponding test, to determine the level of migration of chloride ions into the UHPC over 90 days. According to these findings, the chloride ion content was extremely low for all curing regimes. The average chloride content for different curing regimes was less than 0.00312 lb/ft^3 and the average value in most cases was 0.00125 lb/ft^3. All of these values are below the minimum accuracy threshold for the test method, indicating that the volume of chlorides that penetrated into the UHPC was extremely low. A summary of average values at various durability parameters for UHPC, HPC, and NC is presented in Table 2. In addition, the durability properties of UHPC, HPC, and NC are compared in graphical form in Figure 4.

Table 2. Durability properties of UHPC compared to HPC and NC

| | | HPC | | NC | |
Parameter	UHPC	Value	Ratio to UHPC	Value	Ratio to UHPC
Salt Scaling Mass Lost (28 cycles)	0.010 lb/ft^2	0.031 lb/ft^2	3.0	0.31 lb/ft^2	30
Chloride Ion Diffusion Coefficient	2.2×10^{-13} ft^2/s	6.5×10^{-12} ft^2/s	30	1.2×10^{-11} ft^2/s	55
Chloride Ion Penetration Depth	0.04 in.	0.32 in.	8	0.91 in.	23
Chloride Ion Permeability Total Charge Passed	10 – 25 coulombs	200 – 1000 coulombs	34	1800 – 6000 coulombs	220
Carbonation Depth (3yrs.)	0.059 in.	0.16 in.	2.7	0.28 in.	4.7
Reinforcement Corrosion Rate	4×10^{-7} in./yr	9.8×10^{-6} in./yr	25	4.7×10^{-5} in./yr	120
Abrasion Resistance Relative Vol. Loss Index	1.1 – 1.7	2.8	2.0	4.0	2.9
Resistivity	53.9 kΩ·in.	37.8 kΩ·in.	0.70	6.3 kΩ·in.	0.12

Compiled based on data presented by Lee et al. 2005, Schmidt and Fehling 2005, Roux et al. 1996, Bonneau et al. 1997, Schmidt et al. 2003, Vernet 2004, VSL Proprietary Limited 2003, and Perry and Zakariasen 2004
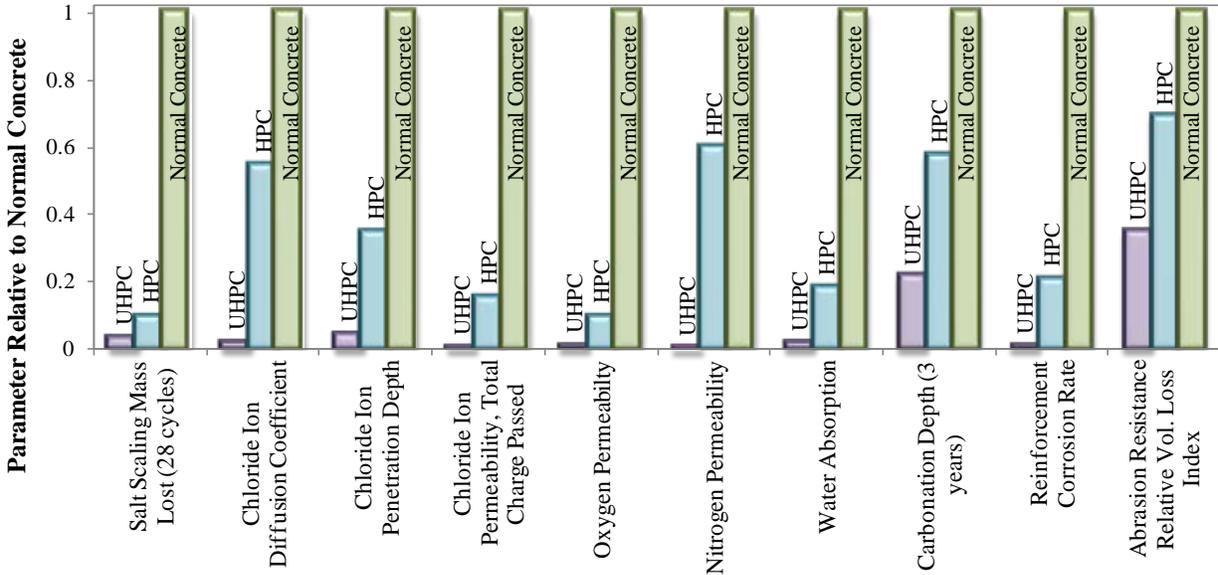
Vande Voort et al. 2008, Institute for Transportation

Figure 4. Comparison of durability properties of UHPC and HPC with respect to normal concrete (lowest values identify the most favorable material)

2.3 Previous Studies on Interface Bond Behavior

New and rehabilitated bridge decks are often constructed with concrete overlays. In order for the deck and the overlay sections to act compositely, horizontal shear forces must be transferred across their interface. Over the past 50 years, many studies have been done and analytical expressions developed to determine both the horizontal shear force along the composite section interface and the horizontal shear capacity of a particular interface. The bond strength between concrete materials cast at two different times is influenced by many factors, including the following:

- Deck surface conditions such as moisture content (wet or dry), roughness, presence of cracking on the deck surface, and cleanliness
- Use of bonding agents (if any) and age of the bond
- Strength and thickness of the overlay material
- Surface roughness and preparation methods

Zilch and Reinecke (2001) proposed that the shear strength of a concrete-to-concrete interface can be described using a combination of three different load-carrying mechanisms (Figure 5): adhesion, shear friction, and shear reinforcement.
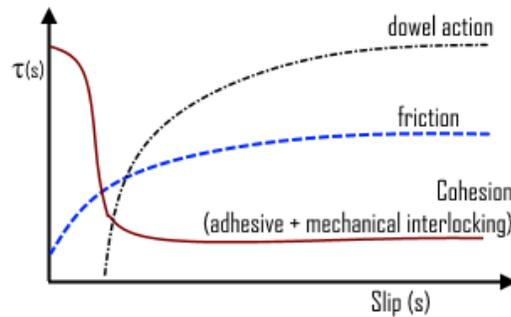
Zilch and Reinecke 2001, Precast/Prestressed Concrete Institute

Figure 5. A schematic view of the load carrying mechanisms at the concrete-to-conrete interface

The adhesion component is initiated by chemical bonds established between the particles of the old and new concrete. Thus, the adhesion component is influenced by the composition of the overlay mix, especially by a mix incorporating supplemental cementitious materials. When the shear stress reaches the maximum adhesion capacity, debonding between the substrate and the overlay occurs at the concrete-to-concrete interface, and the shear stresses will be transferred by mechanical interlocking generated by surface roughness. If the interface is subjected to compression, the shear stresses will be transferred by shear friction. With the increase of the relative displacement between concrete layers, the reinforcement that crosses the interface will be subjected to tensile forces and induce compression at the interface, thereby increasing the shear friction component. Due to the relative slip along the interface, the shear reinforcement will also be subjected to shear, usually called dowel action.

2.3.1 Hanson (1960)

Research performed by Hanson in 1960 included a study that investigated composite action between precast concrete girders and cast-in-place deck slabs. Two main types of interface shear tests were developed by Hanson (1960) in this research. First, push-off tests directly measured the shear capacity of an interface between two concretes by creating a shear force between two compositely or monolithically cast concrete blocks. Second, tests of composite beams created shear across the cold joint interface between a precast beam and a cast-in-place deck by bending the composite beam in flexure. A total of 62 push-off specimens and 10 precast T-shaped girders were tested to investigate the horizontal shear mechanism. Test variables of this study included the effects of adhesive bonds, roughness, keys, and stirrups. Concrete compressive strengths ranged from approximately 3000 psi to 6000 psi. Since then, different variations of the same types of tests have been used by several researchers and are the basis for the majority of the existing shear friction research. Key findings of this investigation included the following:

- Concrete strength dictated the initial peak values for all specimens tested. However, the influence of concrete strength was not systematically investigated as part of this study.

13

- The depth of the roughness at the interface had no effect on the shear carrying capacity of the section. Push-off tests were shown to be valuable in determining the strength of the horizontal shear connection for composite action.

Based on these experimental observations, Hanson (1960) proposed a design expression for the interface shear stress capacity with the form

$$v_u(\text{psi}) = A_o + 17500\rho \tag{1}$$

where A_0 is a constant and ρ is the reinforcement ratio across the interface.

Calibrating this equation with the experimental results, A_0 was found to be 500 psi and 300 psi for rough and smooth surfaces, respectively. Hanson (1960) further concluded that roughened bonded contact surfaces were the only advisable interface between precast beams and cast-in-place slabs.

2.3.2 Birkeland and Birkeland (1966)

Birkeland and Birkeland (1966) were the first to propose a linear expression to evaluate the ultimate shear stress carrying capacity of concrete interfaces. They proposed a shear friction hypothesis for explaining the mechanics of interface shear transfer as the resistance provided by friction across a roughened surface. The friction force is therefore the product of the normal clamping force across the interface and the tangent of the contact angle. The proposed expression is as follows:

$$v_u = \rho f_y \mu \tag{2}$$

where v_u is the ultimate longitudinal shear stress at the interface, ρ is the reinforcement ratio, f_y is the yield strength of the reinforcement, and μ is the coefficient of friction. This is the basic form of the equation currently used by both American Concrete Institute (ACI) in their code ACI 318 (2011) and the American Association of State Highway and Transportation Officials (AASHTO) in their load resistance factor design (LRFD) guidelines for bridges (AASHTO 2010). The coefficient of friction was empirically determined and varied depending on the surface preparation of the interface between the two concretes. Birkeland and Birkeland (1966) suggested (1) $\mu = 1.7$ for monolithic concrete (i.e., friction angle of 59.5º), (2) $\mu = 1.4$, for artificially roughened construction joints (i.e., friction angle of 54.5º), and (3) $\mu = 0.8$ to 1.0 for ordinary construction joints and for concrete-to-steel interfaces (i.e., friction angle of 38.7º to 45.0º). (See Figure 6)
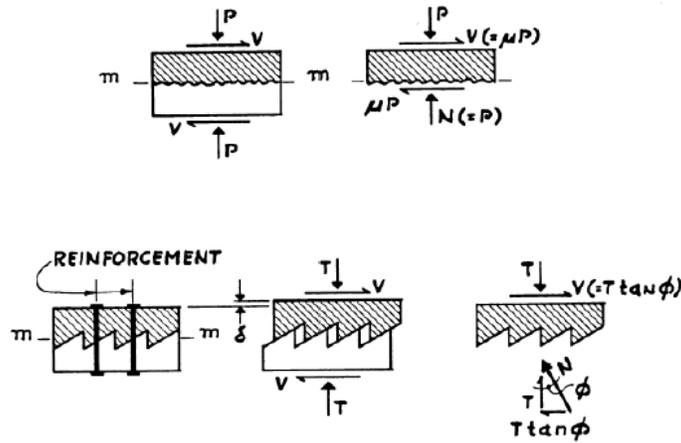
Figure 6. A saw tooth model proposed by Birkeland and Birkeland (1966) for shear friction

2.3.3 Saemann and Washa (1964)

Saemann and Washa (1964) tested a total of 42 composite T-beams with different interface roughness and varying interface shear reinforcement. The beams were designed to experience large interface shear stresses before they failed in flexure. The concrete in the web and flanges was poured at two different times, and a 1/8 inch deep surface finish was provided along the interface. The composite T-beams were tested under a four-point bending configuration. The horizontal shear stress at the interface was calculated using the basic VQ/Ib equation. Following the experimental results, an equation for the ultimate shear strength for a rough interface with interface reinforcement was proposed.

$$v_u = \frac{2700}{\left(\dfrac{x}{d}+5\right)} + 17500\rho \frac{\left(33-\dfrac{x}{d}\right)}{\left(\dfrac{x}{d}\right)^2 + 6\left(\dfrac{x}{d}\right) + 5} \tag{3}$$

where x is the shear span, d is the effective depth, and ρ is the interface reinforcement ratio.

2.3.4 Badoux and Hulsbos (1967)

Badoux and Hulsbos (1967) proposed a design expression to predict the ultimate longitudinal (i.e., along the interface length) shear strength as a sum of two terms, with the first representing the contribution of the natural bond between two different age concretes and the second representing the contribution of the reinforcement crossing the interface. The experimental tests on composite beams included two different types of finishing surfaces at the interface. An intermediate surface roughness was obtained by applying a retarding agent on the fresh concrete and applying a steel brush to the surface one day after casting. The rough surfaces at the interface

15

were created using either a board having a protruding nail or a metal plate with teeth. Based on the experimental results, the following equations were proposed to estimate the interface shear capacity.

For intermediate finish construction joints:

$$v_u = \frac{2000}{\left(\dfrac{x}{d}+11\right)} + 20000\rho \tag{4}$$

For rough construction joints:

$$v_u = \frac{3500}{\left(\dfrac{x}{d}+11\right)} + 20000\rho \tag{5}$$

where x is the shear span; d is the effective depth; and ρ is the interface reinforcement ratio.

2.3.5 Mattock (1981)

Mattock (1981) investigated the behavior of concrete-to-concrete interfaces under cyclic loading. The main goal of these tests was to determine how the design expressions developed for monotonic loading should be modified in order to be used for cyclic loading. Two design expressions developed by this researcher and his co-workers, Mattock and Hawkins (1972) and Mattock et al. (1976), for both normal and lightweight concrete were adopted to assess the ultimate longitudinal shear stress at the interface of composite specimens under cyclic loading.

Mattock (1981) suggested that the shear strength of the concrete-to-concrete interface under cyclic loading should be considered equal to 0.8 of the shear strength under monotonic loading for monolithic specimens made of normal and lightweight concrete and for rough interfaces between concrete parts cast at different ages. If the bond between concrete parts is destroyed, the shear strength under cyclic loading should be calculated as 0.6 of the shear strength under monotonic loading. The shear transfer mechanism of composite specimens after cracking, using both monotonic and cyclic loading, was found to be identical to that of monolithic specimens.

2.3.6 Walraven, Frénay, and Pruijssers (1987)

In order to test concrete strength, Walraven et al. (1987) developed a large experimental study with 88 push-off specimens and proposed a non-linear function to predict the shear strength of initially cracked interfaces. This design expression, including the reinforcement ratio, the yield strength of the reinforcement, and the concrete compressive strength, is as follows:

$$v_u = 15.7\left(f_c'\right)^{0.406}\left(0.007\rho f_y\right)^{0.0353\left(f_c'\right)^{0.303}} \tag{6}$$

where $f_c^{'}$ is the concrete compressive strength.

This design expression is based on a model proposed by Walraven (1981) in which the concrete is represented by the binding paste and the aggregates (assumed as spheres) and where the interface between them is considered to be the weakest zone.

2.3.7 Mattock (1988)

Mattock (1988), in a discussion about the paper by Walraven et al. (1987), presented a modified design expression incorporating the normal stress at the interface. In this new expression, the first term represents the shear strength due to cohesion and the second term represents the shear strength due to friction between aggregates. The modified expression is as follows:

$$v_u = 4.5\left(f_c^{'}\right)^{0.545} + 0.8\left(\rho f_y + \sigma_n\right) \leq 0.3 f_c^{'} \tag{7}$$

where σ_n is the normal stress at the interface. The ultimate longitudinal shear stress is limited to the maximum value of $0.3\,f'_c$.

2.3.8 Randl (1997)

Randl (1997) made one of the most significant contributions to improving the accuracy of the design expressions for assessing the ultimate longitudinal shear stress at concrete-to-concrete interfaces. Following Birkeland and Birkeland (1966) and Walraven et al. (1987)'s work, Randl (1997) presented a design expression that explicitly includes the contribution of cohesion, friction, and dowel action. Cohesion is related to the interlocking between aggregates, friction is related to the longitudinal relative slip between concrete parts and is influenced by the surface roughness and the normal stress at the shear interface, and dowel action is related to the flexural resistance of the shear reinforcement crossing the interface. The first two terms are clearly related to the Coulomb shear friction hypothesis, while the third term represents the contribution of the deformation of the shear reinforcement due to the relative slip between concrete parts. The proposed design expression is given as follows:

$$v_u = \tau_{coh} + \mu\sigma_n + \alpha\,\rho\sqrt{f_c^{'}}\sqrt{f_y} \tag{8}$$

where τ_{coh} is the concrete cohesion due to aggregate interlock, μ is the coefficient of friction, σ_n is the normal stress at the interface due to external loading and tension in the shear reinforcement, α is a coefficient to take into account the flexural resistance of reinforcement (dowel action), ρ is the reinforcement ratio, f'_c is the concrete compressive strength, and f_y is the yield strength of the reinforcement.

With the inclusion of partial safety factors, the design expression was presented as follows:

$$v_u = \frac{c\left(f_c^{'}\right)^{1/3}}{\gamma_{coh}} + \mu\left(\rho k \frac{f_y}{\gamma_s} + \sigma_n\right) + \alpha\, \rho \sqrt{\frac{f_c^{'}}{\gamma_c}} \sqrt{\frac{f_y}{\gamma_s}} \quad \leq \beta v \frac{f_c^{'}}{\gamma_c} \tag{9}$$

where c is the coefficient of cohesion, f_{ck} is the characteristic value of concrete compressive strength, γ_{coh} is the safety factor for the cohesion, k is a coefficient of efficiency for the tensile force that can be transmitted to the shear reinforcement, f_{yk} is the characteristic value of the yield strength of the reinforcement, γ_s is the partial safety factor for the shear reinforcement, γ_c is the partial safety factor for concrete, β is a coefficient allowing for the angle of a concrete diagonal strut, and v is a reduction factor for the strength of a concrete diagonal strut. The suggested values for design parameters for different textures are presented in Table 3.

Table 3. Suggested values of design parameters by Randl (1997)

Surface preparation	Surface roughness, R (mm)	Coefficient of cohesion, c	Coefficient of friction, μ		k	α	β
			f_{ck} >20 Mpa	f_{ck} >35 Mpa			
High pressure water blasting	≥ 3 mm	0.4	0.8	1.0	0.5	0.9	0.4
Sand-blasting	≥ 0.5 mm	0.0	0.7	0.7	0.5	1.1	0.3
Smooth	0	0.0	0.5	0.5	0	1.5	0.2

The adopted partial safety factors are 1.15 and 1.50 for steel and concrete, respectively. Randl (1997) proposed a value of 2.00 for the safety factor of concrete cohesion because this factor is strongly influenced by the surface preparation.

2.3.9 Papanicolaou and Triantafillou (2002)

Papanicolaou and Triantafillou (2002) developed an experimental study consisting of a total of 126 push-off specimens tested under monotonic loading to investigate the shear transfer capacity of interfaces between high performance concrete and concrete with volcanic aggregate. Specimens with interface lengths of 7 in. and 9 ½ in. were tested. The study included the following parameters: (1) compressive/tensile strength of the volcanic aggregate concrete, (2) ratio of shear reinforcement crossing the interface, (3) interface length, (4) surface preparation, (5) lateral confinement, and (6) loading rate. The rough surfaces at the interface were prepared with a special hammer, while the smooth surfaces were prepared using an abrasive disk. Based on the experimental results, the following equation was proposed for estimating the interface shear strength:

$$v_u = \mu\left(\rho f_y + \sigma_n\right)^b + c\left(f_{ct}\right)^d \tag{10}$$

18

where μ is the coefficient of friction, ρ is the reinforcement ratio, f_y is the yield strength of the reinforcement, σ_n is the normal stress at the interface due to external loads, f_{ct} is the mean tensile strength of concrete, and c is a generalized cohesion term. The values proposed for the coefficients b and d and for the coefficients of friction and interface sizes are shown in Table 4.

Table 4. Coefficient of friction and cohesion

Size-surface preparation $b = 1, d = 0.5$	Coefficient of friction μ	Coefficient of cohesion c
Small-smooth	0.33	3.63
Small-rough	0.45	2.97
Large-smooth	0.33	2.33
Large-rough	0.45	1.90

2.3.10 Mansur, Vinayagam, and Tan (2008)

Mansur et al. (2008) investigated the shear transfer across a crack using analytical methods and experimental testing. A single curve formulation was proposed by Mansur et al. (2008) based on the design expression developed by Mau and Hsu (1988) and calibrated with a set of 154 test results. The compressive strength of the concrete adopted in the experimental study was between 2.6 ksi and 14.5 ksi, while the normalized clamping forces ($\rho f_y/f_c$) were between 0.02 and 0.39. This led to a trilinear formulation depending on the normalized clamping force value.

$$\frac{v_u}{f_c'} = \begin{cases} 2.5\left(\rho\frac{f_y}{f_c'}\right) & \text{for } \left(\rho\frac{f_y}{f_c'}\right) < 0.075 \\ \frac{0.56}{\left(f_c'\right)^{0.385}} + 0.55\left(\rho\frac{f_y}{f_c'}\right) & \text{for } 0.075 < \left(\rho\frac{f_y}{f_c'}\right) < 0.27 \\ 0.3 & \text{for } \left(\rho\frac{f_y}{f_c'}\right) > 0.27 \end{cases} \tag{11}$$

2.3.11 Santos and Júlio (2010)

Santos and Júlio (2010) performed an experimental study to investigate the influence of several parameters on the bond strength of concrete-to-concrete interfaces, including (1) the preparation of the substrate surface, (2) the differential shrinkage and stiffness between the substrate concrete and the added concrete layer, and (3) the failure mode. The experimental study included slant shear testing and split-tension testing of composite specimens with concretes poured at different times. The slant shear specimens failed in both interface debonding and cohesive failure (monolithic behavior) modes. It was also observed that an increase in the number of cohesive failures corresponded with an increase in the surface roughness of the interface. Also, generally speaking, the bond strength of the interface, mainly in shear, increased as the surface roughness

increased, as expected. Nevertheless, it was also observed that the bond strength increased as the difference in ages between the substrate concrete and the added concrete layer increased, contrary to what was expected. It was also found that the curing conditions have a significant influence on the bond strength of the interface. For the same surface preparation and the same difference in ages between concrete layers, the specimens cured under exterior conditions had lower values in terms of pure shear strength, with an average decrease of 20%. This decrease was caused by the different daily variations in the relative humidity, which have a significant influence on the curing of concrete at early ages. The study also found that the maximum valley depth (R_v) was identified as the texture parameter that best correlates with the bond strength of the concrete-to-concrete interface, both in shear and in tension. To avoid the effect of strong irregularities of texture, Santos (2009) proposed using mean valley depth (R_{vm}) instead of maximum valley depth for predicting the interface shear strength. Using experimental test results, Santos (2009) correlated the texture parameter mean valley depth (R_{vm}) of each surface condition with the coefficients of cohesion and friction. The interface shear strength for different surface conditions can be estimated using the following equations:

$$\upsilon_{ni} = \begin{cases} \dfrac{1.698 R_{vm}^{0.145} f_{ctd}}{\gamma_{coh}}, \text{ when no reinforcement is provided across interface} \\ \dfrac{1.560 R_{vm}^{0.041}}{\gamma_{fr}}\left(\sigma_n + \rho f_y\right), \text{ when reinforcement is provided} \end{cases} \tag{12}$$

where R_{vm} = mean valley depth of texture, γ_{coh} = 2.6; γ_{fr} =1.2, f_{ctd} = tensile capacity of concrete.

2.4 Previous UHPC-NC Interface Studies

2.4.1 Sarkar (2010)

Sarkar (2010) conducted an experimental study to evaluate the bond strength between a UHPC overlay and a normal concrete substrate with different types of surface textures including smooth, low roughness, and high roughness. This experimental study used three different test procedures, including slant shear tests to evaluate the bond strength under compression and shear, split prism tests performed to evaluate the bond strength under indirect tension, and three point bending tests on a UHPC-normal concrete composite specimen to investigate bond failure under flexural loading.

A total of 27 slant shear tests were conducted using 3 in. × 6 in. composite cylinders made using 5,000 psi normal concrete and UHPC provided by Lafarge (i.e., Ductal). In the slant shear samples, the UHPC–NC interface was inclined at an angle of 30º with respect to the longitudinal axis (vertical axis) of the specimen (see Figure 7(a) for the normal concrete shear samples, 7(b) for the composite cylinders, 7(c) for the slant shear test, and 7(d) for examples of failed slant shear samples).

a) Normal concrete half slant shear test
specimens with different surface textures

b) Composite cylinders

c) Slant shear test

d) Failed slant shear samples with partially chipped surface
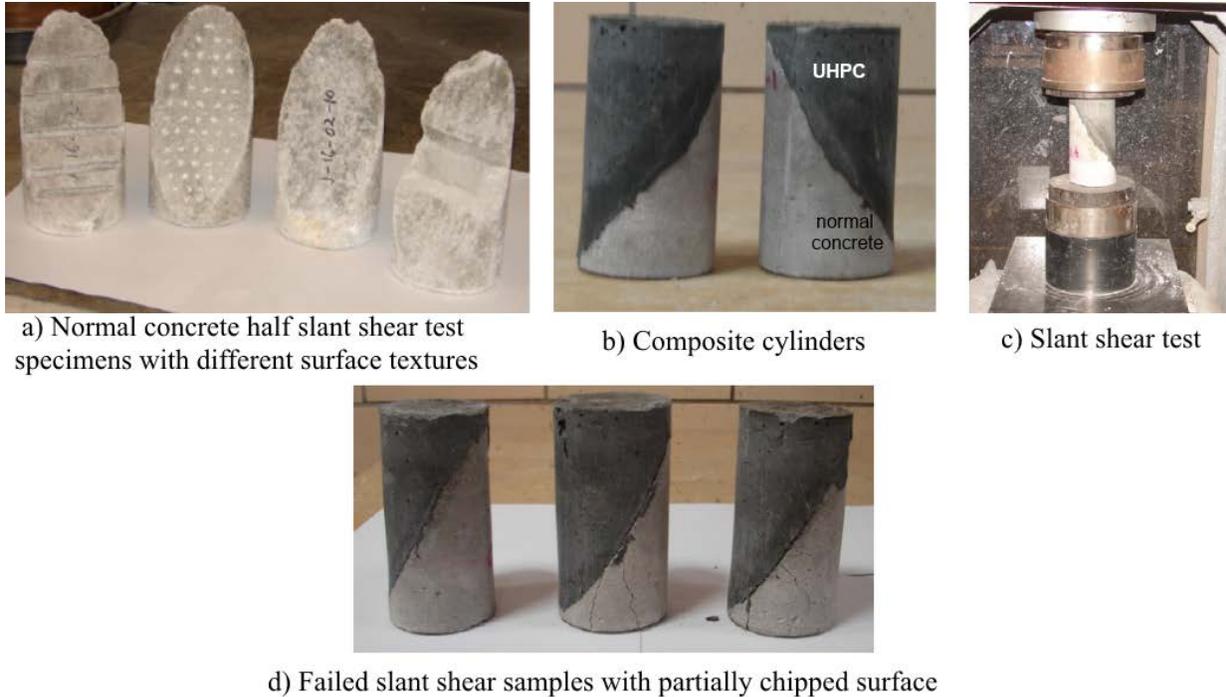
Figure 7. Details of the slant shear specimens tested by Sarkar (2010)

The interface between the UHPC and normal concrete was prepared to represent different roughness and surface preparation methods used in the field. The samples were primarily divided into three categories according to the roughness of the interface surface, including smooth (no surface preparation), medium rough (chipped), and slightly rough surfaces (grooved) with horizontal grooves. The average micro surface depth along the interface was measured using the standard sand patch method, and the texture depth was found to vary from 0.04 in. to 0.1 in. for different roughness. The composite cylinders for the four different types of surface roughness were tested to failure under compression loading. Bond strength was calculated either by dividing the maximum load by the bond area for the specimens that failed along the interface or by dividing the maximum load at failure by the interface area.

The following conclusions were made based on the observations from the slant shear tests.

- For most of the specimens with a smooth interface, the failure occurred along the interface. For the specimens with any kind of surface preparation, the failure propagated into the substrate, with the normal concrete portion of the sample failing under compression. This demonstrates that the bridge deck substrate will be the weakest component of the composite system when using UHPC.

- Under combined compression and shear loading, an average bond strength of 1600 psi was measured for the smooth interface. The partially chipped (medium roughness) and

horizontally grooved specimens resulted in bond strengths that that were 28% and 56 higher than the smooth surface bond strengths, respectively.

Sixteen splitting prism specimens were tested with three different surface textures including smooth, wire brush, and grooved interfaces. The splitting prism samples were 3 in. wide × 3 in. high × 4 in. long, yielding a bond surface area of 12 in^2. The normal concrete strength on the day of the testing was measured to be 5500 psi. All the specimens were tested using the standard testing procedure (see Figure 8(a) for the split-prism samples, 8(b) for an image of the split-prism test equipment, and 8(c) for images of the failed split-prism samples).

a) Split-prism test samples   b) Split-prism test setup   c) Failed Split-prism samples with grooved interface
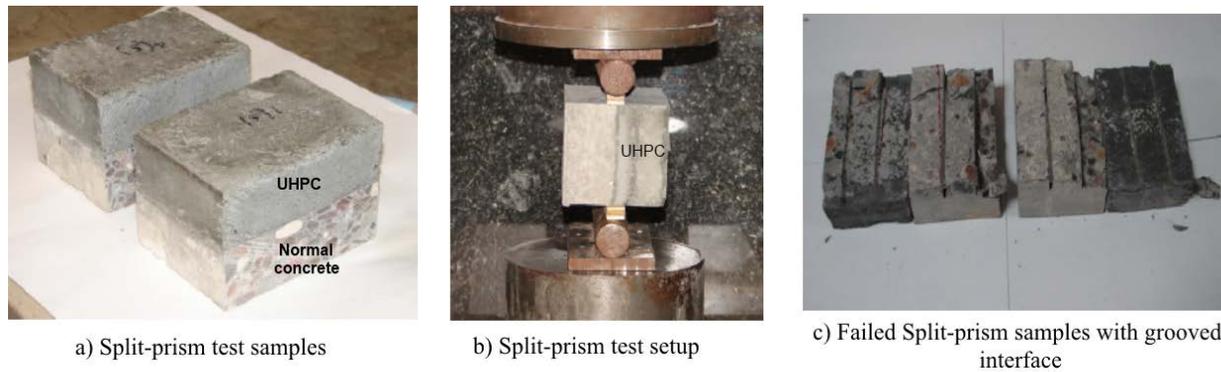
Figure 8. Details of the split-prism specimens tested by Sarkar (2010)

For all the samples, the failure happened at the bond interface on the normal concrete side. The test results showed that the split tensile capacity of a composite UHPC/normal concrete test is not very sensitive to surface roughness. The grooved specimens provided the least bond strength when compared to the smooth surfaces. This was attributed to the fact that, in grooved samples, the groove did not completely fill with UHPC, resulting in air voids within the member and a smaller surface contact area between the two materials.

A total of six composite beam specimens with three different categories of surface textures including smooth surface, horizontal groove, and shear key were tested using a three point bending setup. The composite beam specimens were 16 in. long and 3 in. thick and consisted of equal thicknesses of UHPC and normal concrete. Contrary to the expected field condition for a concrete deck with a UHPC overlay, the flexure tests in the laboratory were performed with the UHPC surface on the bottom (in tension) and the normal concrete on the top (in compression). This was done because the samples were small and no reinforcement was provided. Shear stresses ranging from 150 to 200 psi were calculated along the interface at the flexural failure. Based on the results of the experimental program, it was concluded that UHPC can achieve adequate bond strength to normal concrete surfaces as long as good surface preparation is ensured at the interface.

2.4.2 Banta (2005)

In a Virginia DOT-sponsored study that analyzed the horizontal shear transfer across UHPC produced by Lafarge (i.e., Ductal) and a lightweight concrete interface, Banta (2005) performed a total of 24 push-off tests. Figure 9(a) shows a schematic of the push-off tests, 9(c) shows a the setup, and 9(b) shows surface textures used for the interface between the UHPC and lightweight concrete.

a) Schematic of test specimen details for push-off tests

i) Shear key   ii) 0.5 in. deformed surface   c) Chipped surface

b) Surface textures used for interface between UHPC and light-weight concrete

c) Test setup used for push-off tests
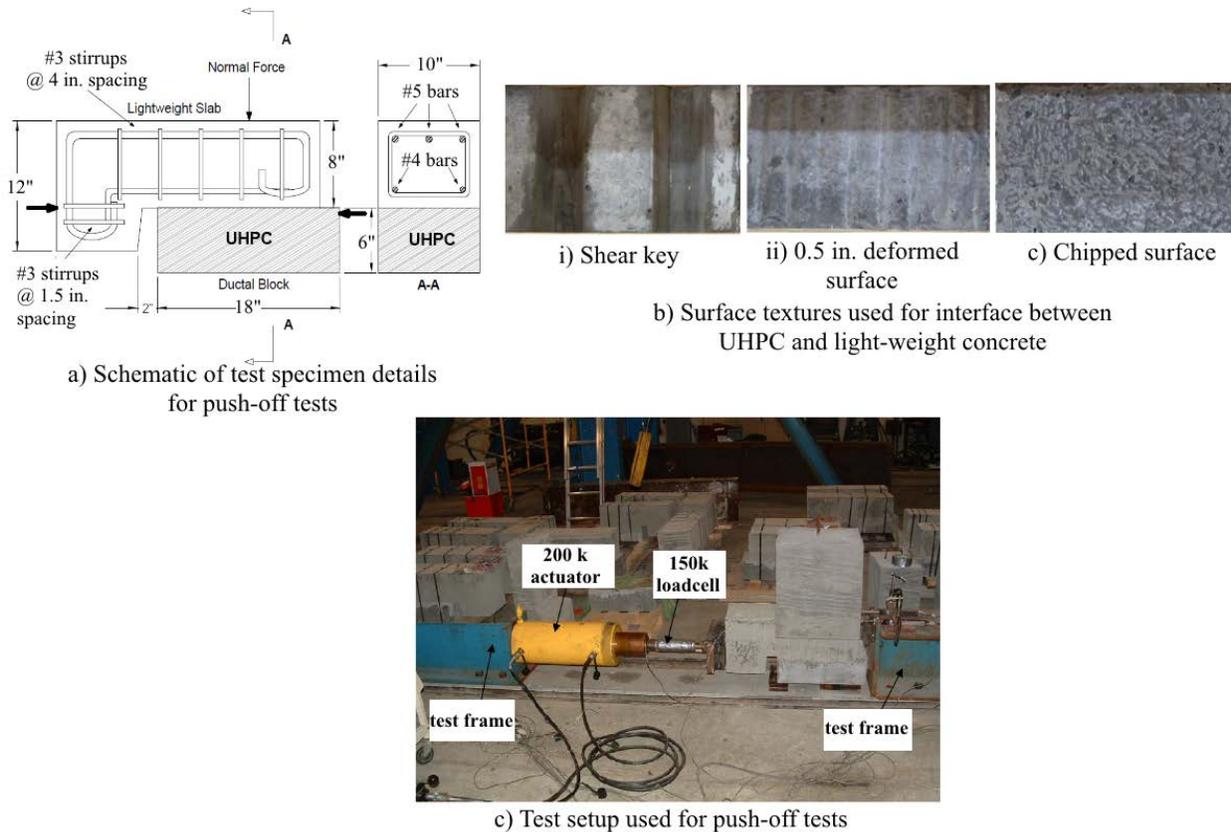
Figure 9. Push-off testing of UHPC-Light Weight Concrete (LWC) specimens by Banta (2005)

Twelve shear connector details were tested with two samples for each detail. The specimens varied in size, reinforcement ratio, and surface conditions. For each size specimen, a specific dead weight block provided a normal force across the interface area. Upon loading each specimen to failure, the load and slip were measured and recorded. The strain in the shear connectors was also measured and recorded for the specimens with interface shear reinforcement. Each specimen consisted of both UHPC and lightweight concrete. The UHPC blocks represented the top flange of the precast UHPC concrete bulb-tee beams that are to be utilized in the construction of the actual bridge in Virginia.

There were three surface treatments consisting of (1) shear keys, (2) ½ in. deformations at 2 in. on center, and (3) chipped surfaces that were investigated to understand the influence of interface

roughness and construction details on shear transfer between a UHPC precast girder and a deck, as shown in Figure 9(b). The shear key texture was formed using 2 in. × 4 in. lumber with angled cuts running lengthwise along each side. The shear keys were 10 in. long, 1.5 in. deep, and 3 in. wide. To mimic the raking of the surface that is typically done on girder tops, ½ in. quarter-round tacked to a sheet of plywood on 2 in. centers was placed on top of the UHPC immediately after it was poured. After the UHPC blocks reached a compressive strength of around 30 ksi, a jackhammer was used to chip the surface. Also, control specimens with smooth surfaces were cast. These specimens had surfaces representative of the actual top flange of the precast beam. These "smooth" blocks had no formed surface deformations, and the UHPC in each block was allowed to self-level. After the UHPC gained its full strength, lightweight concrete was poured. Once the lightweight concrete achieved adequate compressive strength, all the formwork was removed and the specimens were tested using the setup shown in Figure 9.

The forces acting on the specimens were almost directly in line with the interface between the lightweight slab and the UHPC block. Each specimen was able to hold an increasing amount of horizontal load up to an initial cracking load, at which point the initial bond between the concrete at the interface was released. For the specimens with no horizontal shear reinforcement across the interface, this was the ultimate load, and the load- carrying capacity of the interface became negligible.

The following conclusions were drawn based on the experimental results and comparisons with the design equations provided by AASHTO (2010).

- The maximum shear stress across the interface for specimens with no interface shear reinforcement ranged from 102 psi to 400 psi depending on the surface preparation. For the smooth surface, the interface shear capacity varied between 102 psi and 227 psi. The average interface shear capacity for 0.5 in. deformed, keyed, and chipped surfaces was found to be 175 psi, 290 psi, and 355 psi, respectively. The chipped surface condition showed higher capacity compared to other surface preparations due to bonding between the lightweight concrete and exposed fibers in the UHPC.

- For the reinforced specimens, the initial cracking at the interface was not the ultimate horizontal load applied during each test. The shear reinforcement across the interface was engaged upon cracking and subsequently provided a clamping force to the interface, resulting in increased shear transfer capacity until the rebar fracture.

- The interface shear reinforcement experienced a minimal amount of strain prior to the initial separation of the interface, indicating that it made no contribution towards shear capacity before the debonding of the interface.

- The AASHTO (2010) standard specifications provided the most conservative results. The ACI 318 (2014) design equations yielded the least conservative results but were still acceptable for design.

2.4.3 Crane (2010)

In a Georgia DOT-sponsored project designed to evaluate the use of UHPC for prestressed bridge girders, an experimental study was conducted by Crane (2010) to quantify the shear capacity of a UHPC and HPC interface simulating the connection between UHPC girders and a HPC deck. The experimental study included (1) push-off tests on specimens made from HPC cast against UHPC, (2) three-point bending tests on small-scale composite T-beam specimens with UHPC in the web and HPC in the flanges, and (3) large-scale tests on precast, prestressed UHPC bridge girders with cast-in-place HPC decks.

A total of 20 push-off tests were conducted to evaluate the interface shear capacity between precast UHPC and cast-in-place HPC. The primary variables considered in this study were interface surface preparation and interface reinforcement ratio. Three surface preparations for the UHPC/HPC interface were investigated. The first interface used a 1/4 in. deep form liner to create a fluted texture in the UHPC to represent a typical raking surface on top of a prestressed girder. In the second interface, a mildly rough surface was created using burlap placed on the cast UHPC. The third surface was a smooth, as-cast, cold joint surface. The push-off samples included interface shear reinforcement with zero, one, two, or three two-legged No. 3 stirrups across the interface to give reinforcement ratios of 0%, 0.25%, 0.5%, and 0.75%, respectively. The composite specimens for the push-off tests were manufactured by casting one-half from the same UHPC. After this half had cured, the other half was cast against the cold joint using HPC. The measured compressive strengths of HPC and UHPC were 12,200 psi and 28,900 psi, respectively. For all specimens, the interface shear plane was a rectangular section having a width of 7.25 in. and a length of 12 in.

All push-off specimens were tested under monotonic loading using the setup illustrated in Figure 10a. The relative slip movement across the interface was measured at center of the interface on both faces of the specimen. In general, the UHPC/HPC specimens with no interface shear reinforcement experienced sudden failures at much lower loads compared to specimens with interface shear reinforcement. The shear failure occurred through HPC shear keys created by the fluted UHPC interface (see Figure 10b).
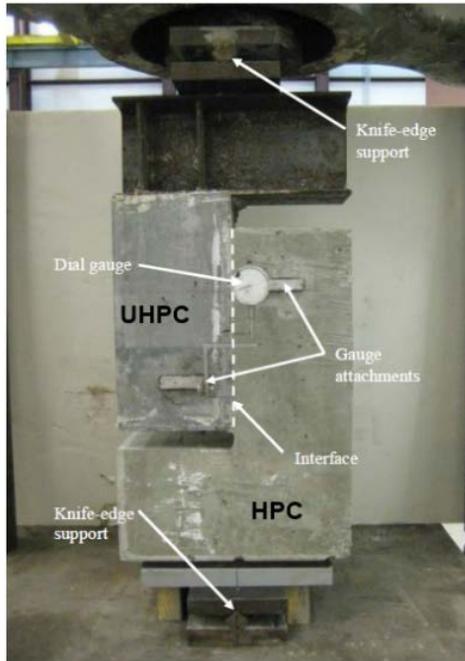
a) Typical test setup for push-off test of a UHPC-HPC composite specimen

b) Failure interface of specimen with fluted surface and no interface reinforcement

Figure 10. Push-off testing of UHPC-NC composite specimen by Crane (2010)

The average measured value for interface shear capacity for the fluted, mildly rough (i.e., through the use of burlap), and smooth surfaces with no interface reinforcement was 531 psi, 368 psi, and 162 psi respectively. Based on the push-off test results and comparisons with ACI and AASHTO design code equations, the following conclusions were drawn:

- The burlap-roughened surface increased the interface shear capacity over the smooth cold joint by 127%, while the fluted surface increased the shear capacity by 228%.

- For the smooth interface, the shear capacity increases linearly with the increase in the interface reinforcement ratio, validating the applicability of the shear friction theory to UHPC/HPC interfaces when a smooth joint is used.

- Current ACI and AASHTO provisions are conservative for estimating the interface shear capacity of composite UHPC/HPC structures.

A total of five composite T-beam tests were performed to examine the interface shear friction capacity of HPC cast against UHPC under bending, creating a condition similar to what would be experienced in the field. The web was cast using 28,930 psi UHPC and the flange was cast in place using HPC with 12,170 psi strength. The cast-in-place deck slab had a reduced length of 88 in. compared to the 120 in. beam length in order to force an interface shear failure. The cross-section details of the composite specimen is shown in Figure 11. Each beam was 120 in. long

and was tested to failure using a three-point loading setup with a 114 in. span between supports, as shown in Figure 11.
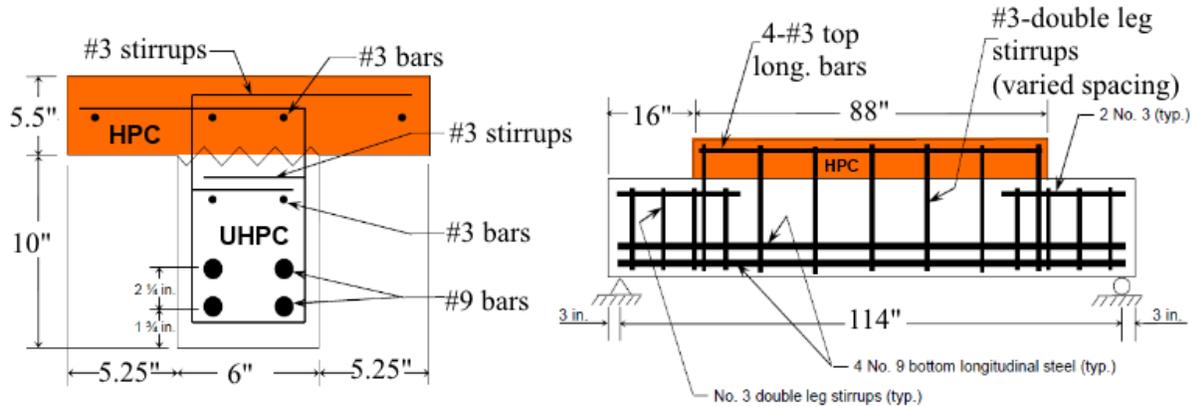
a) Cross-section of composite beam   b) Elevation of the specimen and test setup

Additional labels and orange shading added

Figure 11. Details of UHPC-NC composite beam tests by Crane (2010)

Based on the experimental results and comparing the measured interface shear stresses with push-off test results, the following conclusions were made:

- Smooth, cold joint interfaces should be avoided in design and construction with UHPC where shear forces must be transferred across the interface. Instead, cold joint interfaces between precast UHPC and cast-in-place concretes should be fluted (roughened), which may be accomplished by depressing a form liner into the plastic concrete or by using an equivalent roughening technique.

- For interfaces roughened by at least ¼ in., the AASHTO shear friction guidelines may be used for the design of the interface shear transfer.

2.4.4 Carbonell Muñoz (2012)

Muññoz (2012) investigated the interface bond characteristics of UHPC and normal strength concrete using a variety of bond tests, including the slant shear, splitting prism, and pull-off configurations. The influence of the surface preparation treatment, pre-wetting conditions, and freeze-thaw cycles on the interface bond behavior were investigated.

The first stage of the experimental investigation included splitting tensile tests of composite specimens. A total of 90 composite and 14 monolithic specimens with five different surfaces, including smooth, brushed, chipped, sandblasted, and grooved, were cast with dry and saturated substrate moisture conditions. The micro texture depths for these surface treatments were estimated using the standard sand patch test and are presented in Figure 12.
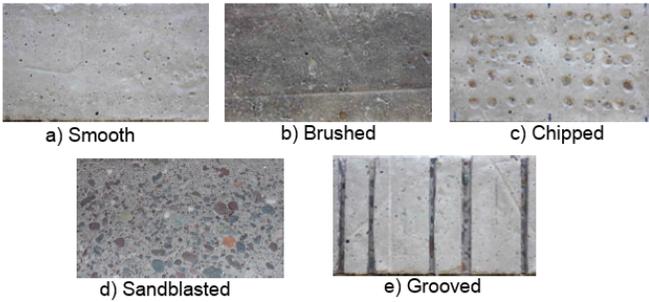
Surface treatment	ICRI Profile	Macrotexture Depth (in)
Smooth	1, 2	0.02
Brushed	1, 3	0.03
Chipped	Not applicable	0.04
Sandblasted	4, 5	0.04
Grooved	Not applicable	Not applicable

a) Different surface textures used for splitting tensile samples

b) Measured microtexture depth of textures used for splitting tensile samples

Figure 12. Details of the split-tensioin testing specimen by Carbonell Muñoz (2012)

Three samples per surface texture were subjected to an increasing number of freeze-thaw cycles (in steps of 300 cycles) before being tested to failure using a split tensile test to estimate the tensile bond strength of interface as an indirect measure of the long-term performance of the interface under variable environmental conditions. A large percentage of composite specimens were cast with the dry, old substrate, but nevertheless achieved excellent bond performance for samples with saturated concrete substrate, indicating the effect of substrate moisture condition on interface bond development. On the basis of results from this test, it was concluded that for sandblasted, chipped, and smooth surfaces the predominant failure occurred in concrete with few failures along the interface through mixed bond failure mode. In the grooved specimens, the failure occurred in the normal concrete grooves. The prolongation of freeze-thaw cycles beyond 300 cycles did not affect the interface tensile bond strength.

Following the tensile splitting tests, a series of slant shear tests were done on composite specimens comprised of UHPC and normal strength concrete mixes. The main aim of the slant shear tests was to study the bond strength at eight days at four different degrees of roughness in the concrete substrate and two different interface angles (60° and 70°). Four different surface textures, brushed, sandblasted, grooved, and roughened (exposed aggregate), and three different normal strength concrete mixes were investigated as part of this stage of testing. The measured compressive strengths of the normal concrete mixes were 6460 psi, 6607 psi, and 8112 psi, respectively. The details of the textures used for the UHPC and NC interfaces are shown in Figure 13. The composite specimens were cast by pouring UHPC on top of the moist cured, saturated, normal strength concrete blocks with slanted interface with predefined surface preparations. All of the samples were subjected to compression at the standard loading rate of 35 psi/second using a Baldwin CT 300 hydraulic load frame (see Figure 13f).

Surface treatment	ICRI Profile	Macrotexture Depth (in)
Brushed	1,3	0.03
Sandblasted	4,5	0.03
Grooved	Not applicable	Not applicable
Rough	Aggregate exposure >8,9	0.09

e) texture depths

(a) Rough surface.

(b) Sandblasted

(c) Brushed surface.

(d) Grooved surface.
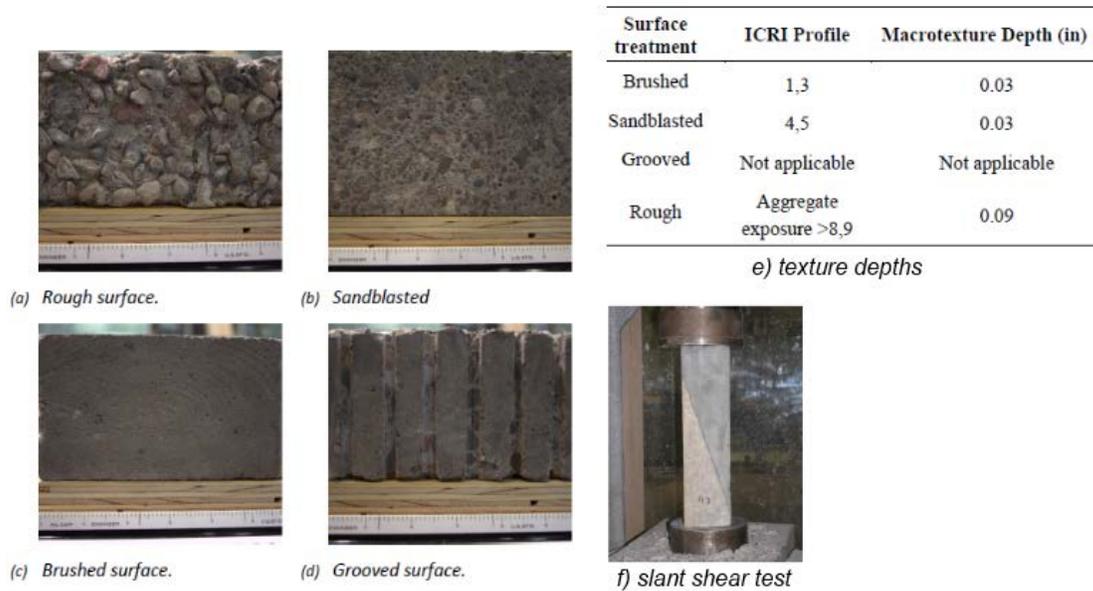
f) slant shear test

Copyright 2012 Miguel Ángel Carbonell Muñoz

Figure 13. Details of interface textures and slant shear tests done by Carbonell Muñoz (2012)

The following observations and conclusions were presented based on Carbonell Muñoz's slant shear testing:

- A total of six different failure modes, including bond failure, mixed failure along the interface, and failure in normal concrete, were observed during testing. All specimens at the age of eight days with an interface angle of 60° failed in the concrete substrate, whereas the specimens with an interface angle of 70° experienced sliding failures. This observation indicates the strong influence of the interface angle on the bond strengths of the interfaces. A higher angle with respect to the horizontal plane produced a more severe state of shear and compression stresses.

- The average bond strengths measured using a 70° interface angle for brushed, sandblasted, grooved, and roughened textures were found to be 1757 psi, 2124 psi, 1634 psi, and 1765 psi respectively.

- The bond capacity at 8 days for all surface preparations exceeded the requirements specified by ACI 546.3R-06 at 7 days and satisfied the minimum bond requirements for 28 days.

3   LABORATORY TESTING

3.1   Introduction

To a large degree, the performance of an overlay material is dependent on how well the overlay material bonds to the concrete substrate. An experimental study to evaluate the bond strength between UHPC and a conventional normal concrete was performed in two phases. In Phase 1 of the testing, five different types of surface textures representing low roughness (< 0.06 in.), medium roughness (0.12 in.), and high roughness (0.2 in. to 0.25 in.) were prepared to evaluate the influence of surface roughness on bond strength. Slant shear testing was conducted to evaluate the bond strength under combined compression and shear loading. After the Phase 1 testing, three-point bending tests were also performed on large-scale UHPC-NC composite specimens replicating bridge decks to investigate the interface behavior before experiencing failure.

This chapter summarizes the experimental program, including materials used, test specimen design and fabrication, details about the textures investigated, test setup, and test results. Test results are presented using key variables such as the applied force, slip, and interface stresses at the peak load. Discussion of the test results and analysis of the test data are presented in subsequent sections.

3.2   Phase I Testing

3.2.1 Specimen Design and Construction

The primary focus of this research project was to characterize the bond strength between a UHPC and normal concrete interface and evaluate the influence of surface roughness on the bond strength between the two materials to further understand the potential application of UHPC as an overlay on bridge decks. As discussed in the previous chapter, there are many test methods available for assessing the bond performance between two different concrete materials. For this research program, the slant shear test was selected for evaluation of the bond characteristics at the normal concrete and UHPC interface.

The experimental program included 60 slant shear specimens and investigated the direct shear transfer across the interface of concrete with different strengths, normal concrete and UHPC, cast at different times and under different conditions. The test variables included the compressive strength of normal concrete, the shear interface surface texture, the curing condition, and the pouring sequence. All specimens had a cold joint provided along the shear plane of the specimen. Considering the practical implementation of the overlay concept, mechanical connections such as shear studs or interface shear reinforcement across the UHPC and NC interface were not considered for experimental evaluation. Based on previous experimental studies of the bond behavior of composite specimens incorporating UHPC (Sarkar 2010) and the slant shear test concept, all interface tests were completed using prismatic members. A test matrix consisting of five different textures and three concrete strengths was used to examine the

feasibility and the effects of different interface textures, concrete strengths, casting sequences, and curing conditions (fully cured versus partially cured vs. wet conditions) on the shear friction behavior of the composite deck interface. The details of the test matrix are summarized in Table 5. UHPCw and UHPCh represent wet-cast UHPC and heat-treated UHPC, respectively.

Table 5. Summary of UHPC-NC interface test matrix

Specimen Type	Texture (# of specimens)	Casting Sequence	Target NC Strength
UHPCw-NC5	5 textures (3 per texture)	Wet UHPC over cured NC	5 ksi
UHPCw-NC7	5 textures (3 per texture)	Wet UHPC over cured NC	7 ksi
UHPCw-NC10	5 textures (3 per texture)	Wet UHPC over cured NC	10 ksi
UHPCh-NC5	5 textures (3 per texture)	Wet NC on heat-treated UHPC	5 ksi

Each UHPC-NC composite specimen was 4.5 in. × 6 in. in cross-section and 24 in. long and consisted of an inclined joint with different interface textures at the mid-height of the specimen. Based on preliminary calculations and previous research, an inclination angle of 53.1° to the horizontal axis was chosen to ensure that sliding along the interface would be the primary failure mode (Zilch and Reinecke 2000). The joint interface surfaces were prepared using five different form liners of varying roughness, as shown in Figure 14.

a) TR 6: 2/61 thames (Reckli) (1.26 mm)   b) TR 5: 2/102 Parana (Reckli) (1.59mm)

c) TR 2: 2/98 Vltava (Reckli) (3 mm)

d) TR 1: 2/63 Wisla (Reckli) (5 mm)   e) TR 3: Fluted Rib pattern (Fitzgerald) (6.5mm)
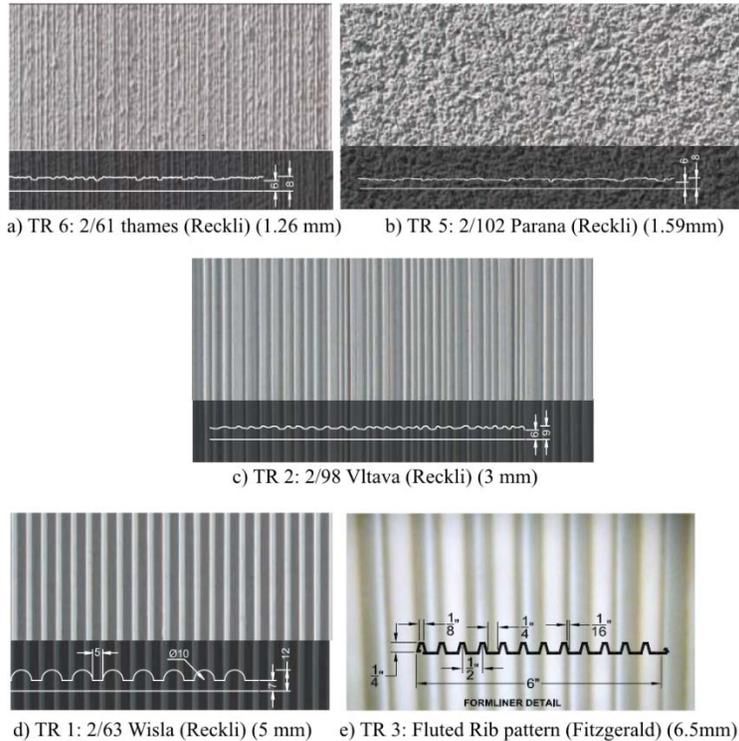
Figure 14. Details of various textures used for the UHPC-NC interface study

These form liners are typically used in the precast concrete industry, primarily for achieving architectural details. The commercial name of the texture, manufacturer details, and typical average texture depths are shown in Figure 14.

The use of form liners ensured consistent interface roughness between units. The roughness of different form liner patterns was chosen to replicate the different surface conditions expected during field applications. The degree of roughness in each case was established based on the macro texture depth, which varied from 2 mm to 6.5 mm for the textures used in this study. In addition, the study investigated the influence of concrete strengths using 5 ksi, 7 ksi, and 10 ksi mix designs.

The composite specimens were cast vertically using concrete mix and standard flexural beam molds with appropriate texture according to the following steps (see Figure 15):
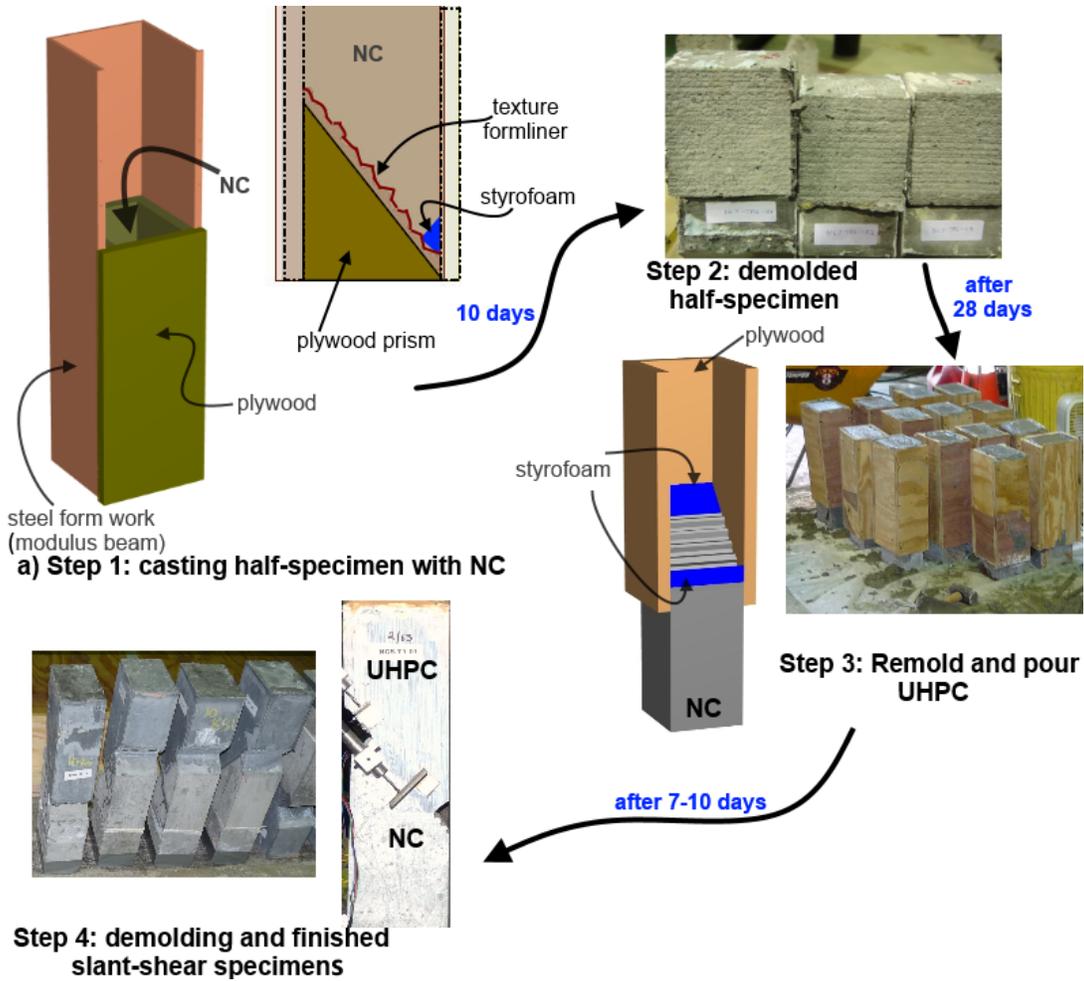
Figure 15. Casting sequence used for NC-UHPC interface slant shear specimens

- Three quarter inch thick plywood pieces were used inside the standard modulus beam steel forms to create the formwork.

- A non-absorbing, thin, poly-vinyl adhesive sheet was applied to all the plywood surfaces that were in contact with concrete (UHPC or normal concrete) to prevent any water absorption from UHPC or normal concrete mix by the wood forms. The use of the adhesive sheet meant that the application of form oil was not required during specimen construction, and the vinyl sheet prevented any accidental contamination of the interface.

- A triangular prism was made using plywood to create the inclined surface for casting. The form liner texture samples were glued onto the top of the inclined wood plane using standard caulk. This entire prism block, including the texture, was placed at the bottom of the form. A triangular Styrofoam piece was used to create the reduced interface length (see Step 1 in Figure 15).

- Normal concrete of different strengths was poured vertically into the forms. The normal concrete had at least 5 inches slump, and a 0.5 in. standard vibrator was used to make sure the concrete was compacted well to create a good textured surface.

- The molds were removed after 7 to 10 days, and the half-specimens made with normal concrete were subjected to normal air curing inside the structural laboratory (see Step 2 in Figure 15).

- At least 28 days after curing, the normal strength concrete half-specimens were placed back into plywood molds with the slant side facing up. Two triangular Styrofoam pieces were placed on the top and the bottom of the interface. The Styrofoam pieces were used to create a reduced interface length and were glued firmly to the plywood using caulk to prevent any seepage of UHPC (see Step 3 in Figure 15).

- All these molds were transported to the Coreslab Structures's precast plant in Omaha, Nebraska, for pouring UHPC. The UHPC was mixed as part of a UHPC pile project.

- All the finished samples were left to air-cure for at least 10 days before they were shipped back to Iowa State University (ISU). The wooden forms were not removed, and all the interface specimens were crated in a tight, rectangular, wooden box to prevent any damage during shipment (see Step 4 in Figure 15).

- The specimens utilizing heat-treated UHPC were created following the same procedure, except that the UHPC was poured first at the precast plant and then subjected to the standard heat treatment process recommended by Lafarge. Concrete made from a normal concrete mix with a 5 ksi compressive strength was then poured on top of the UHPC half-specimen having the appropriate texture. The molds were removed 14 days after pouring the normal concrete, and the specimens were air-cured.

- All the cylinder samples prepared for measuring the strength of concrete mixes were also demolded on the same day as the slant shear specimens and were subjected to air curing. This

was done to keep the curing conditions of the cylinders the same as the curing conditions for the test specimens.

- Depending upon the casting sequence and curing conditions, the interface texture was first created on either the UHPC or the normal concrete half-sections. For specimens with wet UHPC, the normal concrete with specified concrete strength was poured into the mold with the form liner, and these half-sections were then cured for 28 days under ambient conditions. After the curing process, the normal concrete half sections were placed back into molds with the slant side up, and the molds were filled with UHPC to form the other (top) half-section.

- The final composite units were cured under ambient conditions until the day of testing. The slant shear specimens were named according to the surface preparation of the interface, normal concrete strength, and the UHPC casting sequence. Therefore, a typical name for a slant shear sample made with wet UHPC poured on a cured normal concrete half-section was given as [normal concrete mix]-[texture designation]-[specimen number]. For example, NC5-TR1-01 represents slant shear specimen 1, made with 5 ksi normal strength concrete, TR1 texture, and wet UHPC. For all the samples where the normal concrete was poured over a heat-treated UHPC half-section with texture, a prefix "HT" was added to the specimen name to represent the pouring sequence.

3.2.2   Materials

3.2.2.1   Concrete Mix

The concrete mixes used in specimen construction were sourced from local ready mix concrete suppliers or precast producers. The 5 ksi concrete specimens were constructed using a standard Iowa DOT bridge deck mix ordered from a local ready mix plant. The higher strength specimens were fabricated using the standard mix designs at the Coreslab Structures precast plant in Omaha, Nebraska. All the normal concrete mixtures contained Portland cement, water, coarse aggregates, fine aggregates, and high-range water reducers (where applicable). A total of 24 cylinders (4 in. × 8 in. and 6 in. × 12 in.) were used to determine the concrete compressive strengths at 28 days and at the time of slant shear specimen testing. The measured concrete strengths of the all mixes used for slant shear tests conducted in this project are presented in Table 6.

Table 6. Measured compressive strength of normal strength concrete used for slant shear specimen testing

S. No	Mix Designation	Design Strength (psi)	Measured Values	
			28-Day Strength (psi)	Test Day Strength (psi)
1	NC5	5000	5,128	5,200
2	NC7	7000	6,890	7,459
3	NC10	10000	6,230	6,403
4	NC5*	5000	4,618	4,725

* This mix is used for samples with heat-treated (HT) UHPC

Based on the cylinder testing at 28 days, it was noticed that the concrete mix designated as NC10 did not reach the desired compressive strength of 10 ksi. No attempt was made to reproduce these specimens since the measured NC 10 mix had compression strength between other two mixes. The NC10 specimens as cast were still used in the research project, as the goal of testing was to investigate the effect of concrete strength on the interface bond strength.

3.2.2.2 UHPC

UHPC manufactured and supplied by Lafarge North America was used for casting the test specimens. The UHPC represented by brand name Ductal JS1000 was mixed using the overhead batch plant mixer at the Coreslab Structures precast plant in Omaha, Nebraska. This specific UHPC mix was chosen because it has been used by the Iowa DOT and because Coreslab Structures was the precast producer for past projects (e.g., UHPC pile foundations [Vande Voort et al. 2008] and UHPC waffle deck system [Aaleti et al. 2011]). Extensive cataloguing of the mechanical and durability characteristics of this material was also done previously for other UHPC related projects at FHWA and Iowa DOT (Aaleti et al. 2011, Bierwagen and Abu-Hawash 2005, Keierleber et al. 2008, Wipf et al. 2009, Rouse et al. 2011). The UHPC material strengths were found to fall between 15000 to 21000 psi at the time of testing.

3.2.2.3 Texture Characterization

The texture depth of the UHPC-NC interface was measured before pouring the second half of the slant shear specimen. The texture depth was measured on three specimens for each texture used in this study. The depth was measured using a caliper for deeper textures (i.e., TR1 to TR3, see Figure 14) or using the standard sand patch test (ASTM E965-96) for shallow textures (i.e., TR5 and TR6, see Figure 14). As part of the sand patch test, 50 cm^3 of calibrated fine sand was spread on the interface surface, the diameter of the circle formed was measured at quarter points, and the resulting average value was determined. The mean texture depth (MTD) was determined using a texture parameter that quantifies the surface texture as follows:

$$MTD = \frac{4V}{\pi D^2}$$

(13)

where V is the volume of sand dropped over the surface (mm³) and D is the average value of the diameter of the area covered by the sand (mm). The details of the textures investigated using the sand patch test are presented in Table 7 along with average values of measured sand patch diameter and texture classification.

Table 7. Details of shallow textures and measured mean texture depth

Serial No.	Texture (Brand)	Sand Patch Diameter (mm)	Average Sand Patch Diameter (D) (mm)	Mean Texture Depth (mm) = $\frac{4V}{\pi D^2} * \times 10^3$
1	TR6: 2/61 Thames	240, 220, 215, 225	225	1.26
2	TR5: 2/102 Parana	200, 195, 200, 205	200	1.59

* $V = 50$ cm³ (volume of the sand used); 1 in. = 25.4 mm

3.2.3 Test Setup and Results

The slant shear test was performed according to the ASTM C882 standard test method (ASTM 2005). This test is typically used to understand the bond strength between hardened concrete and hardened or freshly mixed concrete. The composite slant shear specimens were subjected to uniaxial compression at the ends using a universal testing machine (see Figure 16a), which subjected the interface to shear stresses along the inclined joint interface.

a) Slant shear test setup   b) Premature compression failure in NC   c) Specimen with FRP retrofit for NC
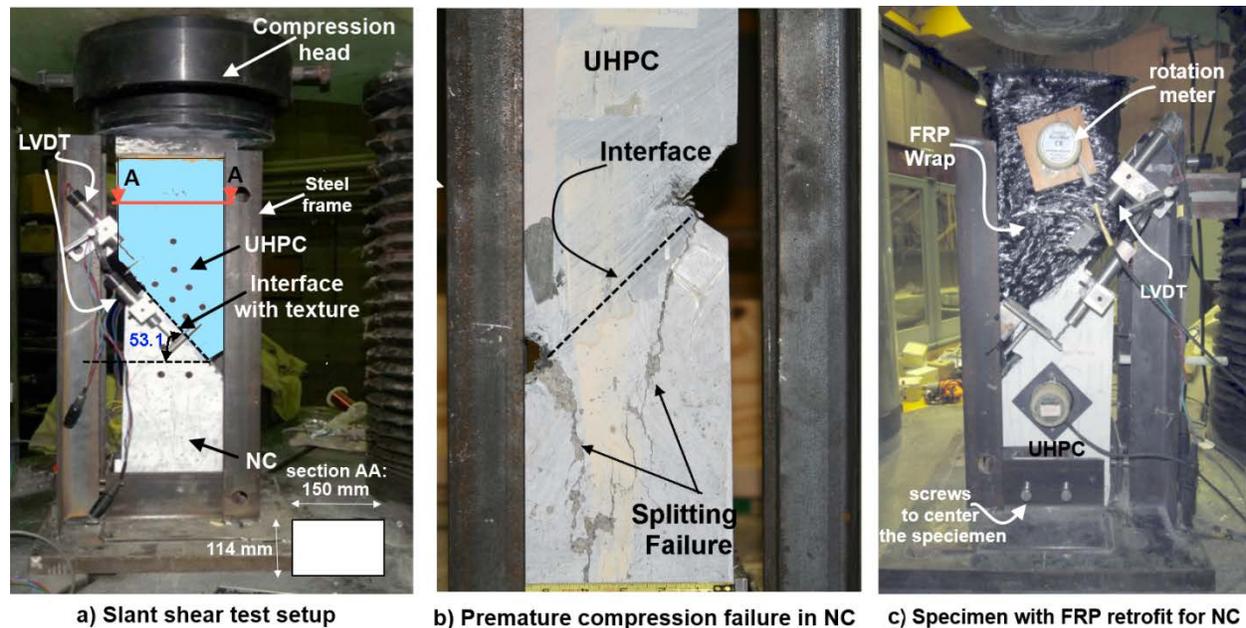
**Figure 16. Slant shear test setup and specimen retrofit**

The specimens were placed into a steel test frame made using standard 3 in. × 3 in. × 1/4 in. L angles welded to a 1 in. thick plate (Figure 16a). This test frame was designed to prevent the top

half of the specimen from experiencing free fall if the interface completely fails and was designed to help with the leveling and centering of the specimen in the uniaxial compression machine. Several instruments, including displacement transducers and rotation meters, were attached to the test specimen in the interface region to adequately characterize the specimen's performance and to closely monitor the movement along the inclined shear interface.

A total of four linear variable differential transducers (LVDTs) were placed along the length of the interface to capture the slip at this location. Two rotation meters were also attached, one on each half of the specimen, to monitor any rotation induced by possible eccentricity of loading. The inclination of the interface for all the samples was measured using an electronic level. The exact interface length and thickness were measured using a caliper, and the measured values are presented later in Table 8. All the specimens were subjected to uniaxial compression loading under displacement control until the load was dropped by 20% from the measured peak load. The data from all instruments were acquired using MegaDAQ at a rate of one sample per second.

During the first series of tests on the NC5-TR specimens, it was observed that specimens with deeper textures failed prematurely before the interface experienced significant sliding due to the formation of splitting cracks in the normal concrete. These cracks initiated at the ends of the interface and propagated into the normal concrete (see Figure 16b). In order to prevent such premature failures, samples with deeper textures were retrofitted with fiber-reinforced polymer (FRP) wrap as shown in Figure 16c.

The normal concrete section of the composite specimen was wrapped with FRP fabric glued to the specimen with high-strength, two-part epoxy. The FRP strengthening was expected to confine the normal concrete and prevent the splitting cracks from damaging the NC part of the specimen as they did in earlier tests.

All 60 slant UHPC and NC interface specimens were tested to failure, failure due either to significant slip at the interface or to splitting of the NC. Generally, the specimens failed by experiencing sliding along the interface. However, in a few specimens with deeper textures, even after the FRP retrofit, the splitting of the NC took place prior to the sliding interface failure. In specimens that failed under the sliding failure mode, the failure surface was located within the interface of the normal concrete and the UHPC or in the normal concrete adjacent to the interface boundary. The normal concrete between the UHPC ridges along the interface failed under combined shear and compression stresses, leading to the sliding failure along the interface. In the specimens with deeper textures that failed under sliding, normal concrete was left between the ridges, as shown in Figure 17c and Figure 17d, indicating that the interface behavior is exclusively dictated by the strength of the normal concrete and that the behavior of interface can be predicted based on the normal concrete shear strength at the interface.
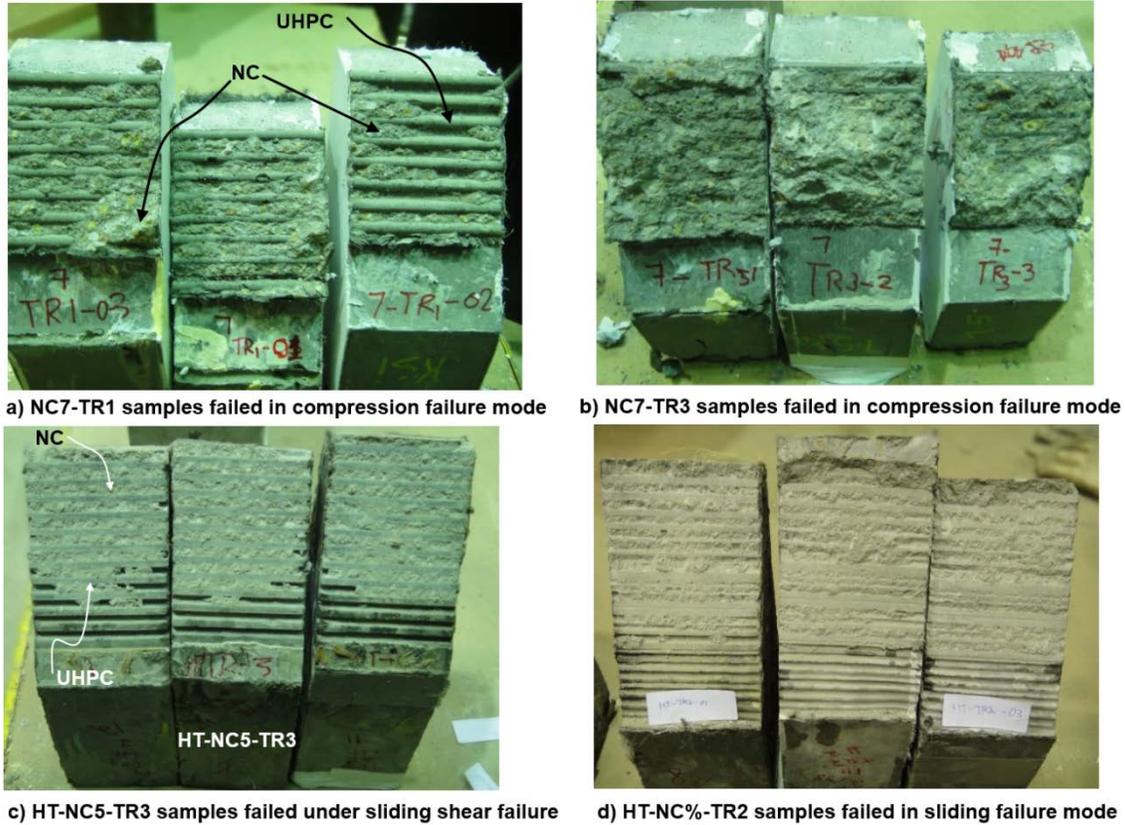
Figure 17. Samples of UHPC-NC interfaces of specimen with different failure modes

For the specimens where the failure occurred in the normal concrete substrate rather than at the interface, indications are that the bond strength is greater than the strength of the substrate concrete. The failure mode of each tested sample was visually examined and classified as a bond failure or a concrete substrate compression failure.

The interface bond strength was calculated by dividing the maximum load along the inclined plane by the interface contact area. This method gives the exact interface bond strength for specimens that failed in a sliding failure mode and indicates the minimum interface bond strength for those specimens that failed in the substrate concrete when experiencing compressive failure. The normal stress applied to the interface is also calculated by dividing the normal component of the applied load by the interface contact area. The calculated interface shear stress values for all slant shear specimens with different concrete strengths and interface textures, along with the observed failure types, are presented in Table 8.

Table 8. Summary of slant shear test results

Specimen name	Texture depth (mm)	Texture Name	Thickness (in.)	Interface Length (in.)	Interface Angle (degrees)	Concrete Strength (ksi)	Retrofit	Failure Type	Peak load (kip)	Shear stress (ksi)
NC5-TR6-01			6.0000	3.6250	53.5000	5.2		S	38.4679	1.4217
NC5-TR6-02	1.26	2/61 Thames	6.0000	3.6250	52.5000	5.2		S	49.4164	1.8025
NC5-TR6-03			4.3125	5.2500	51.3000	5.2		S	69.3121	2.3892
NC5-TR5-01			6.0000	3.7500	54.2000	5.2		S	29.6870	1.0701
NC5-TR5-02	1.59	2/102 Parana	6.0000	3.4688	53.0000	5.2		S	80.7989	3.1005
NC5-TR5-03			4.2500	5.3750	52.9000	5.2		S	77.5327	2.7070
NC5-TR2-01			4.2500	5.3750	52.5000	5.2		C	69.9727	2.4301
NC5-TR2-02	3.0	2/98	4.3125	5.5625	51.8000	5.2		C	83.9750	2.7510
NC5-TR2-03			4.3125	5.6250	55.0000	5.2	Yes	C	87.4750	2.9539
NC5-TR1-01			4.2500	5.1250	51.5000	5.2		C	83.0008	2.9822
NC5-TR1-02	5.0	2/63	4.3125	5.5000	52.5000	5.2		C	67.0674	2.2433
NC5-TR1-03			4.2500	5.5000	51.4000	5.2		C	61.7250	2.0637
NC5-TR3-01			4.1875	5.1875	55.4000	5.2		S	55.4500	2.1012
NC5-TR3-02	6.25	Plastic	4.2500	5.4375	52.4000	5.2		C	75.8000	2.5988
NC5-TR3-03			4.2500	5.0625	53.9000	5.2		C	60.7000	2.2795
NC5-TR4-01			4.1250	5.9375	52.7000	5.2		C	71.0500	2.3076
NC5-TR4-02		Vac-u-form	3.7500	6.5000	53.1000	5.2		C	69.0250	2.2645
NC5-TR4-03			4.2500	5.5000	54.0000	5.2		C	61.6000	2.1320
NC7-TR6-01			4.1875	4.875	53.9	7.459		S	82.5125	3.2658
NC7-TR6-02	1.26	2/61 Thames	4	4.46875	53	7.459		S	74.475	3.3275
NC7-TR6-03			4.125	4.4375	53.7	7.459		S	66.475	2.9268
NC7-TR5-01	1.59	2/102 Parana	4.125	4.65625	53.3	7.459		C	100.9875	4.2156
NC7-TR5-02			4.125	5	53.3	7.459		C	78.6875	3.0589
NC7-TR2-01			4.1875	4.6875	54.8	7.459		C	118.1125	4.9170
NC7-TR2-02	3.0	2/98	4.25	4.75	53	7.459		C	103.0125	4.0753
NC7-TR2-03			4.25	4.75	53.6	7.459	Yes	C	64.1125	2.5562
NC7-TR1-01			3.875	4.75	52.6	7.459		C	97.175	4.1941
NC7-TR1-02	5.0	2/63	4.375	4.625	51.8	7.459		C	77.6625	3.0162
NC7-TR1-03			4.4375	4.6875	56.7	7.459		C	86.3625	3.4702
NC7-TR3-01			4.25	4.5625	54.7	7.459		S	76.9375	3.2382
NC7-TR3-02	6.25	Plastic	4.3125	4.3125	54	7.459		C	94.5625	4.1136
NC7-TR3-03			4.25	4.53125	53.4	7.459		C	94.8	3.9520
NC10-TR6-01	1.26	2/61 Thames	4.2500	5.0000	52.4000	6.403	Yes	S	66.7250	2.4878
NC10-TR6-02			4.0000	3.7500	53.4000	6.403	Yes	S	50.4375	2.6995

Specimen name	Texture depth (mm)	Texture Name	Thickness (in.)	Interface Length (in.)	Interface Angle (degrees)	Concrete Strength (ksi)	Retrofit	Failure Type	Peak load (kip)	Shear stress (ksi)
NC10-TR6-03			4.2500	4.3125	53.9000	6.403	Yes	C	N/A	N/A
NC10-TR5-01	1.59	2/102 Parana	4.1250	5.0000	49.2000	6.403	Yes	S	91.3750	3.3537
NC10-TR5-02			4.2500	4.8750	51.0000	6.403	Yes	S	79.2250	2.9717
NC10-TR2-01			4.2500	5.2500	54.0000	6.403	Yes	C	118.9500	4.3129
NC10-TR2-02	3.0	2/98	4.2500	4.8750	52.6000	6.403	Yes	S	79.6750	3.0550
NC10-TR2-03			4.3125	4.7500	52.8000	6.403	Yes	S	40.1500	1.5612
NC10-TR1-01			4.3125	4.5000	52.7000	6.403		C	69.0500	2.8304
NC10-TR1-02	5.0	2/63	4.2500	4.5625	53.3000	6.403	Yes	S	133.8750	5.5355
NC10-TR1-03			4.2500	4.5000	51.4000	6.403	Yes	C	100.4375	4.1043
NC10-TR3-01			4.3750	5.0000	52.6000	6.403	Yes	C	90.7625	3.2961
NC10-TR3-02	6.25	Plastic	4.3125	4.5000	55.4000	6.403	Yes	C	86.0625	3.6504
NC10-TR3-03			4.1875	5.1250	51.3000	6.403	Yes	C	104.6375	3.8052
HT-NC5-TR6-01			4.1250	5.5000	51.7000	4.725	Yes	S	52.9000	1.8298
HT-NC5-TR6-02	1.26	2/61 Thames	4.2500	5.5000	52.7000	4.725	Yes	S	69.2500	2.3566
HT-NC5-TR6-03			4.3750	5.1875	50.3000	4.725	Yes	S	64.5375	2.1879
HT-NC5-TR5-01	1.59	2/102 Parana	4.1250	5.2500	51.7000	4.725	Yes	S	33.4750	1.2131
HT-NC5-TR5-02			4.1875	5.2500	51.4000	4.725		C	72.8375	2.5893
HT-NC5-TR2-01			4.2500	5.3125	53.4000	4.725	Yes	S	71.2125	2.5321
HT-NC5-TR2-02	3.0	2/98	4.1250	5.1250	53.3000	4.725	Yes	S	54.6750	2.0736
HT-NC5-TR2-03			4.1250	5.2500	53.8000	4.725	Yes	S	81.4125	3.0336
HT-NC5-TR1-01			4.3750	5.3125	54.4000	4.725	Yes	S	64.0250	2.2398
HT-NC5-TR1-02	5.0	2/63	4.1875	5.6875	54.8000	4.725	Yes	S	93.9125	3.2222
HT-NC5-TR1-03			4.1250	5.5000	50.6000	4.725	Yes	S	93.4750	3.1837
HT-NC5-TR3-01			4.2500	5.0000	53.7000	4.725	Yes	S	87.2750	3.3100
HT-NC5-TR3-02	6.25	Plastic	4.1250	5.0000	51.9000	4.725	Yes	S	85.3125	3.2550
HT-NC5-TR3-03			4.2500	4.9375	51.3000	4.725	Yes	S	67.6875	2.5174

S = sliding failure, C = compression failure, Retrofit = Yes implies strengthening using FRP, N/A = text data was not recorded due to malfunction of DAQ

.

A comparison of the average interface bond capacity normalized with normal concrete strength for each surface roughness and concrete strength is presented in Figure 18 and Figure 19.
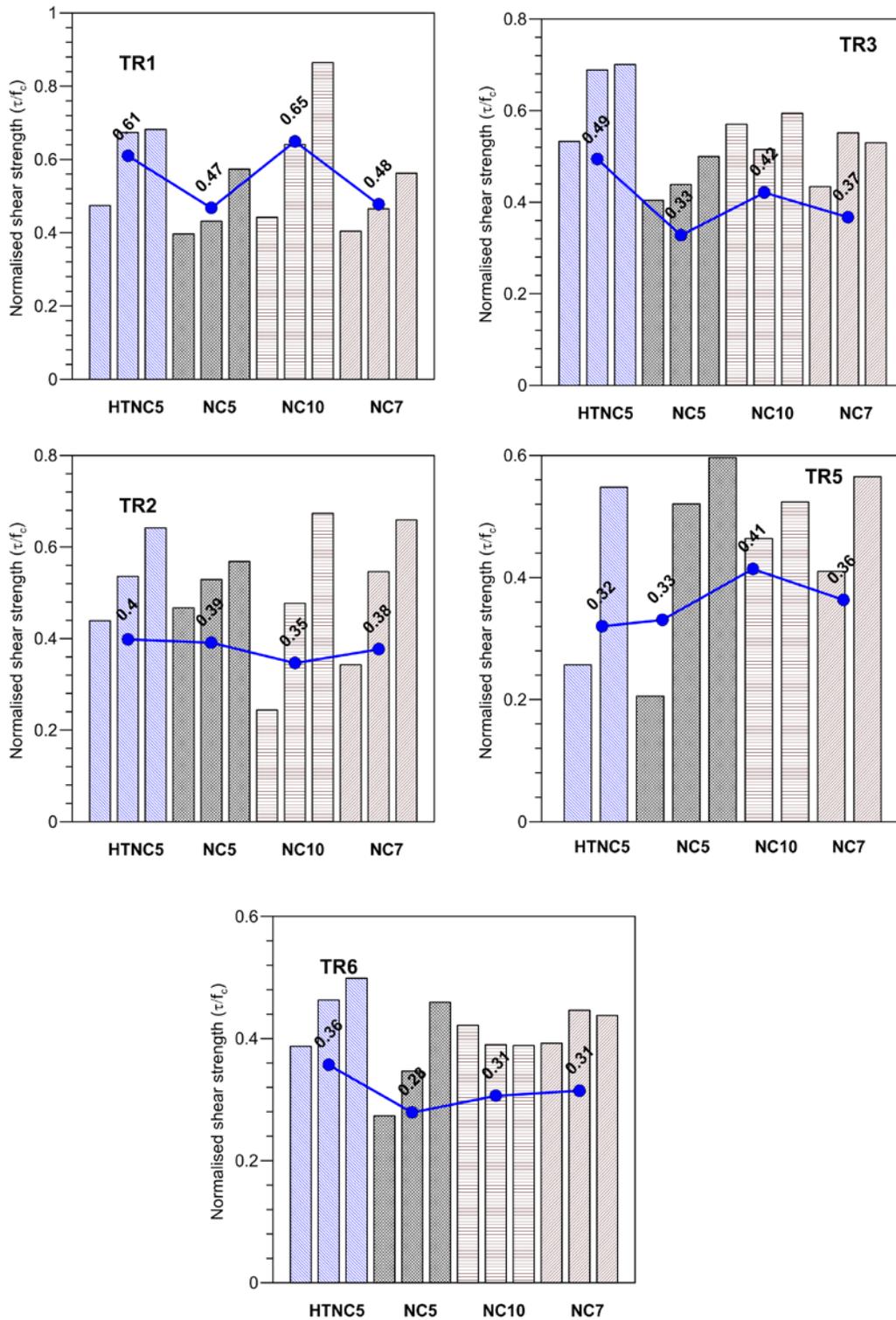

Figure 18. Normalized interface bond strength for different textures and concrete strengths
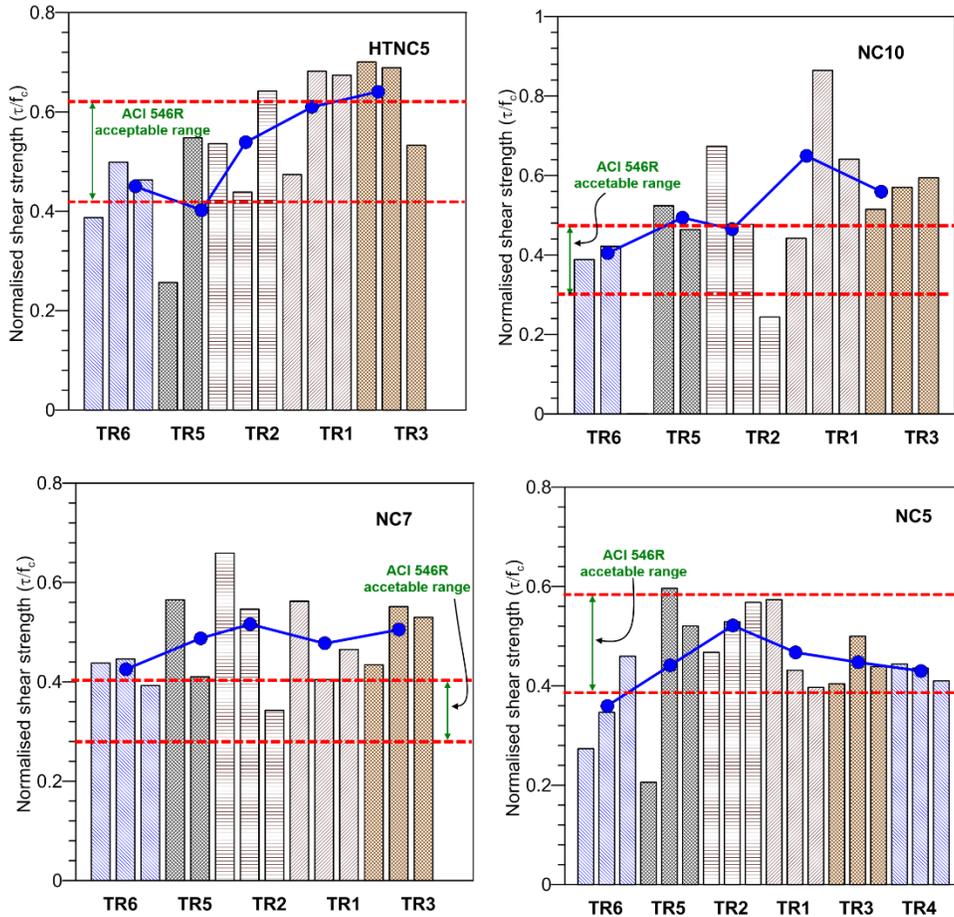
Figure 19. Comparison of interface bond strength with texture depth and concrete strength

The bond strength generally increased with the increase of texture roughness and concrete strength. The casting sequence, however, did not significantly influence the bond strength. In Figure 19, the measured bond strength values are compared to the ACI specified bond strength range that is recommended for selecting repair materials in the Guide for the Selection of Materials for the Repair of Concrete (2004) (ACI 546R-04). It is clear that the average interface bond strength was within the acceptable limits for textures deeper than 2 mm for all concrete strengths. However, the average bond strength values for TR5 and TR6 textures (having a texture depth of less than 1.6 mm) are below the recommended values when a 5 ksi normal strength concrete mix was used. Because most bridge decks are constructed using 4 to 5 ksi concrete mix, it might be prudent to use an interface texture depth of more than 1.6 mm (= 1/16 in.) to create a good interfacial bond between a UHPC overlay and normal concrete. The interface strength values were normalized with respect to concrete strength and the square root of the concrete strength and are plotted for different textures in Figure 20.
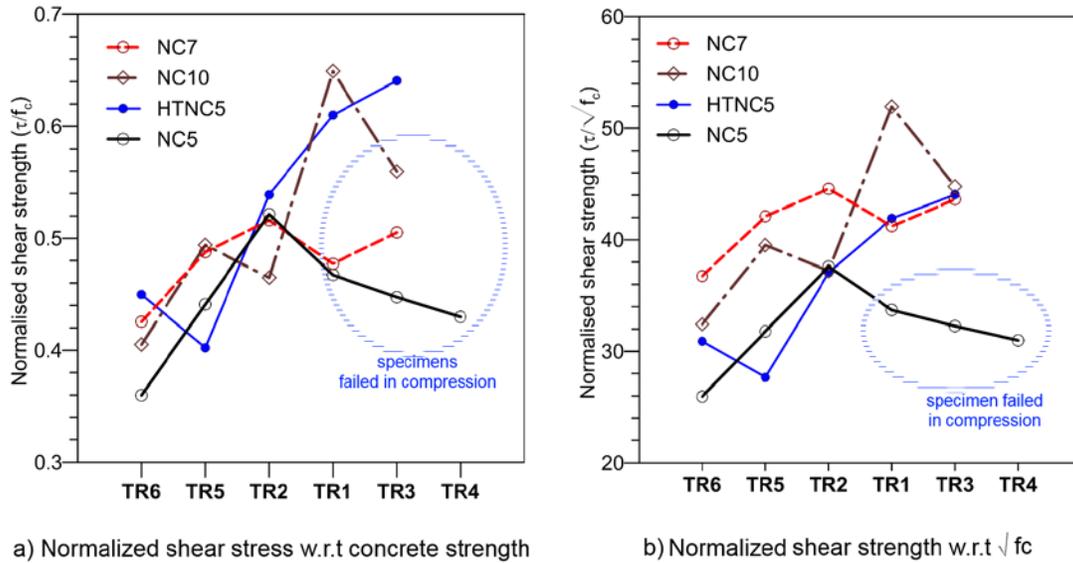
Figure 20. Variation of normalized interface bond strength for different textures

From Figure 20a, it is clear that the interface shear strength depends on the concrete strength and increases with increased concrete strength for a given texture depth. Figure 20 can also be interpreted as indicating an increase in adhesion between NC and UHPC with increased concrete strength. Figure 20 also suggests that a clear trend for interface shear strength that can be represented by a simple mathematical equation cannot be obtained without including the normal stress on the interface. Also, the shear friction theory by Birkeland (1986) and Section 5.8.4 of the AASHTO LRFD Bridge Design Specifications (2010), which addresses the interface shear strength capacity at the girder-to-deck interfaces, suggests that the interface shear strength is a function of normal strength and adhesion between materials. According to the shear friction theory, the interface shear capacity should be related to normal force and adhesion in the following format:

$$v_{ni}(\text{psi}) = c(\text{psi}) + \mu\sigma_n(\text{psi}) \tag{14}$$

where v_{ni} = nominal interface shear resistance [psi], c = cohesion factor (the effects of cohesion and/or aggregate interlock), μ = friction factor, and σ_n = compressive normal stress on the shear plane.

AASHTO (2010) (Section 5.8.4) guidelines suggest the following:

- For normal-weight concrete placed against a clean surface, free of laitance, with the surface intentionally roughened to an amplitude of 0.25 in., $c = 0.24$ ksi, $\mu = 1.0$, and v_{ni} should not exceed the lesser of $0.25f'_c$ and 1.5 ksi.

- For concrete placed against a clean concrete surface, free of laitance but not intentionally roughened, c = 0.075 ksi, $\mu = 0.6$, and vni should not exceed the lesser of $0.2f'_c$ and 0.8 ksi.

43

For all tested textures, Figure 18 shows that the measured interface shear strength was higher than the values calculated as per the AASHTO (2010) guidelines. However, to capture the measured cohesion and friction factor, the variation of the measured interface shear strength as compared to the normal stress on the interface for different textures is plotted in Figure 21.
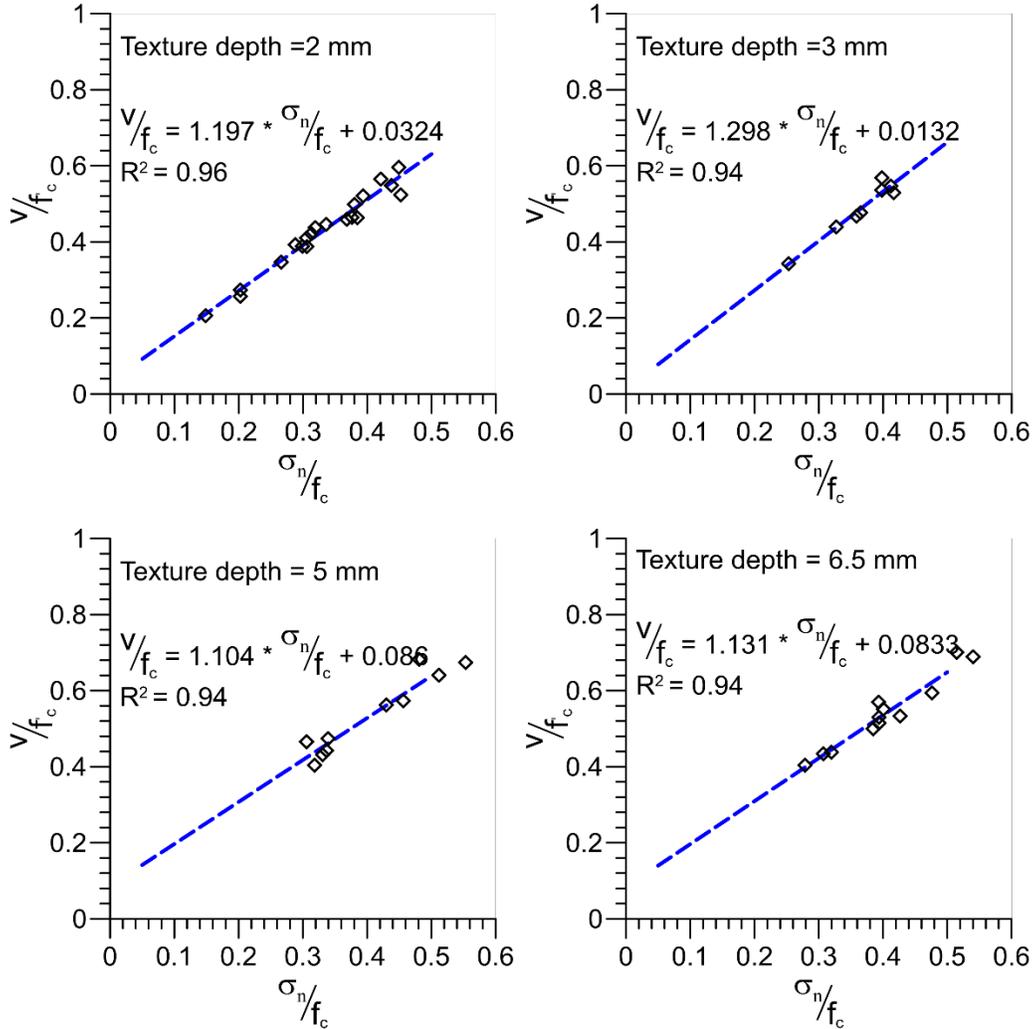
Figure 21. Normalized interface shear strength vs. normal stress for different texture depths

By fitting a linear curve to the observed experimental values, the adhesion and friction coefficient values for different texture depths and concrete strengths were obtained. The cohesion factor increased with the texture depth and concrete strength.

It was found that the minimum value of the cohesion factor for a 6.5 mm texture (TR3) was 0.395 ksi, which is higher than the required AASHTO- minimum value of 0.24 ksi. For other textures with texture depths of less than 0.25 in., the lowest value of cohesion was found to be 0.063 ksi, which is slightly less than the AASHTO-specified value of 0.075 ksi. However, the average cohesion value for these textures was around 0.26 ksi, much higher than the AASHTO

recommended value of 0.075 ksi. The coefficient of friction value varied between 1.104 and 1.298, depending on the texture depth. The low coefficient of friction value for deeper textures can be attributed to the fact that most of the specimens failed in compression mode rather than shear sliding mode. These values, then, could be used to set lower boundaries for design purposes. The average value for the friction factor for the shallow textures with a depth of less than 5 mm (i.e., textures TR5, TR6, and TR2) is 1.2, which is twice the value specified by AASHTO. These observations suggest that the AASHTO recommendations provide a conservative estimate for the UHPC-NC interface shear capacity and could be used for design purposes.

There are also a number of empirical and semi-empirical equations proposed in the literature to calculate the strength of concrete-to-concrete interfaces that are subjected to longitudinal shear stresses based on shear friction theory. A comparison between experimental test results from the slant shear testing and the calculated shear strength based on the equations presented in Table 9 is shown in Figure 22.

Table 9. Design equations for interface shear strength in literature (used for comparison)

S. No.	Source	Equation
1	AASHTO 2010	$$\upsilon_{ni} = \min\begin{pmatrix} c + \mu\left(\dfrac{P_c + A_s f_y}{A_{cv}}\right) \\ K_1 f_c' \\ K_2 \end{pmatrix},$$ where: • $c = 0.075$ ksi, $\mu = 0.6$, $K_1 = 0.2$, and $K_2 = 0.8$ ksi for normal-weight concrete, no intentional roughness • $c = 0.24$ ksi, $\mu = 1.0$, $K_1 = 0.25$, and $K_2 = 1.5$ ksi for normal-weight concrete, intentionally roughened to amplitude of 0.25 in. • $\left(\dfrac{P_c + A_s f_y}{A_{cv}}\right)$ is the normal stress on the interface (in ksi)
2	Loov 1978	$$\upsilon_{ni} = 0.5 f_c' \sqrt{\left(\dfrac{\rho f_y + \sigma_n}{f_c'}\right)},$$ where: • $\rho f_y + \sigma_n$ is the total clamping stress normal to the interface • f'_c is the concrete strength in psi
3	Walraven et al. 1987	$$\upsilon_{ni}(\text{psi}) = 15.686\left(f_c'\right)^{0.406}\left(0.007\rho f_y\right)^{C_2}; C_2 = 0.0353\left(f_c'\right)^{0.303}$$ where: • ρf_y can be considered to be the clamping force acting normal to the interface
4	Mattock 1988	$$\upsilon_{ni} = 4.5\left(f_c'\right)^{0.545} + 0.8\left(\rho f_y + \sigma_n\right) \leq 0.3 f_c'$$ where: • $\rho f_y + \sigma_n$ is the total clamping stress normal to the interface
5	Tsoukantas and Tassios 1989	$$\upsilon_{ni} = \begin{cases} 0.5\left(f_c'\right)^{2/3}\sqrt{\sigma_n} & \text{for rough surfaces} \\ 0.4\sigma_n & \text{for smooth surfaces} \end{cases}$$
6	Mattock 1994	$$\upsilon_{ni} = \dfrac{\sqrt{\rho f_y}\left(f_c'\right)^{0.73}}{14.25} \leq 0.3\left(f_c'\right)$$
7	Pattnaik 2000	$$\upsilon_{ni} = \begin{cases} 0.55\sqrt{f_c'}\sqrt{\left(\rho f_y + 36\right)} & \text{for intentionally roughed surfaces} \\ 0.5\sqrt{f_c'}\sqrt{\left(\rho f_y + 36\right)} & \text{for not intentionally roughed surfaces} \end{cases}$$

S. No.	Source	Equation
8	Randl 1997	$$\upsilon_{ni} = c\frac{\left(f_c\right)^{1/3}}{2} + \mu\left(\rho k\frac{f_y}{1.15} + \sigma_n\right) + \alpha\rho\sqrt{\left(\frac{f_y}{1.15}\right)\left(\frac{f_c}{1.5}\right)} \leq \beta\upsilon\frac{f_c}{1.5}$$ where: - For texture roughness > 3 mm, $c = 0.4$, $\mu = 0.8$ for $f_c > 20$ Mpa; $=1.0$ for $f_c > 35$Mpa, $k = 0.5$, $\alpha = 0.9$, $\beta = 0.4$ - For texture roughness > 0.5 mm, $c = 0$, $\mu = 0.7$, $k = 0.5$, $\alpha = 1.1$, $\beta = 0.3$ - For smooth texture $c = 0$, $\mu = 0.5$, $k = 0$, $\alpha = 1.5$, $\beta = 0.2$ - For comparison to slant shear test results $$\upsilon_{ni} = c\frac{\left(f_c\right)^{1/3}}{2} + \mu\left(\rho k\frac{f_y}{1.15} + \sigma_n\right) \leq \beta\upsilon\frac{f_c}{1.5}$$
9	Santos and Júlio 2009	$$\upsilon_{ni} = \frac{1.698R^{0.145}f_{ctd}}{\gamma_{coh}}$$ when no reinforcement is provided across interface $$\upsilon_{ni} = \frac{1.560R^{0.041}}{\gamma_{fr}}\left(\sigma_n + \rho f_y\right)$$ when reinforcement is provided where: R = mean valley depth of texture, $\gamma_{coh} = 2.6$, $\gamma_{fr} = 1.2$, f_{ctd} = tensile capacity of concrete
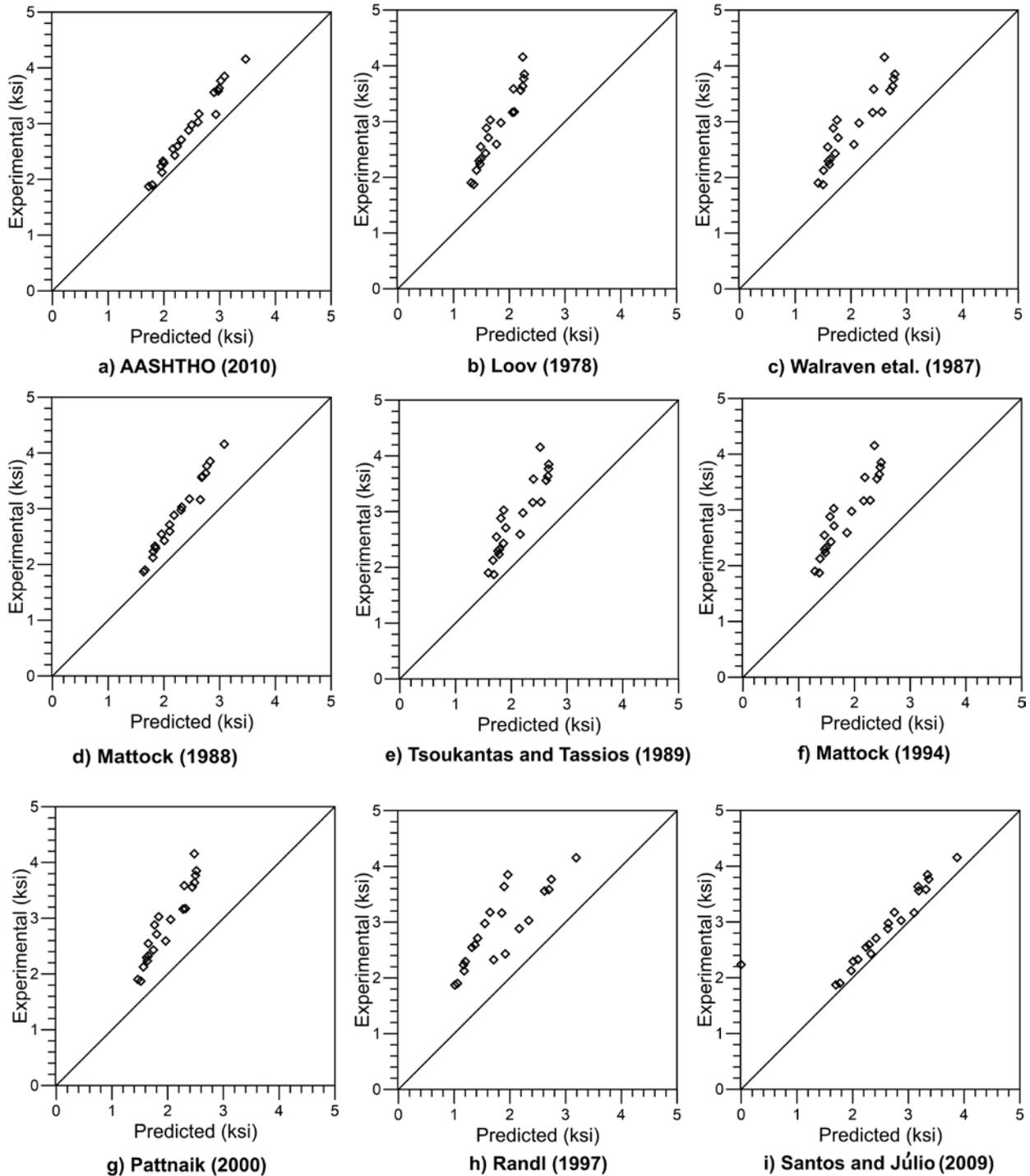
**Figure 22. Comparison of experimental and calculated interface shear strength based on equations in literature**

It is clear from Figure 22 that all the design equations under-predicted the shear strength of the interface. Both the current AASHTO guidelines and the equation proposed by Santos and Júlio (2009) provide a closer estimation of the interface strength compared to the estimations produced

48

by any of the other equations in Table 9. The equation proposed by Santos and Júlio (2009), which takes the interface roughness into account, provided more accurate results than the AASHTO recommendations.

3.3   Phase II Testing

Following the investigation of bond behavior using the slant shear tests on the composite test units in Phase I, four UHPC-NC composite deck specimens with a texture depth varying from 2 mm to 5 mm and a standard overlay composite deck specimen were tested under combined flexural and shear loading.

3.3.1 Specimen Details and Fabrication

A deck region between two adjacent girders, as highlighted in Figure 23(a), was chosen for the experimental investigation. Accordingly, deck panel specimens with dimensions of 2 ft (width) × 8 ft (length) were fabricated at Iowa State University's structural laboratory. The reinforcement in the deck was designed according to AASHTO standards (AASHTO 2010) and was the same reinforcement as is included in current Iowa DOT bridge decks, as shown in Figure 23(b). The cross section of the bridge segment is shown in Figure 23(c).
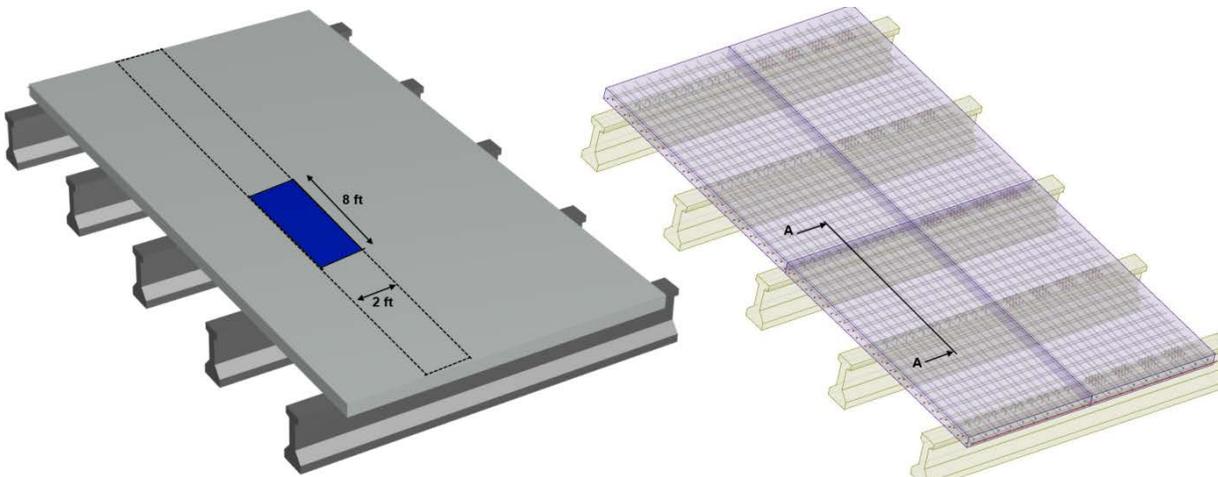
a) Schematic of a typical prestressed concrete girder bridge

b) Transverse and longitudinal reinforcement in a typical bridge deck
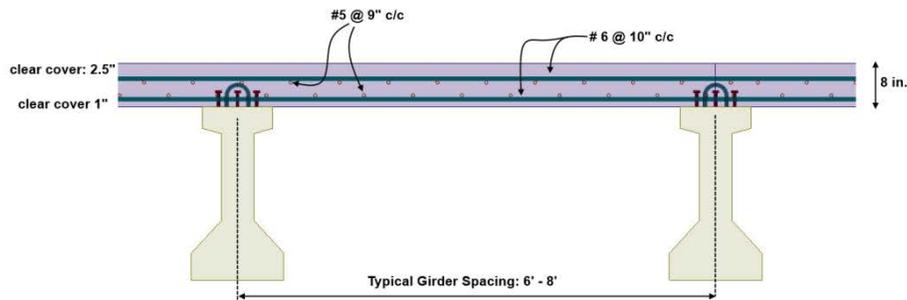
c) Cross-section view of typical bridge deck in the transverse direction (section AA)

Figure 23. Details of a standard Iowa DOT bridge

The interfaces on the top of deck panel specimens were created using TR1 (texture depth: 5 mm), TR2 (texture depth: 3 mm), and TR6 (texture depth: 1.26 mm) form liners as well as a hand broom finish on top of a normal concrete surface. The form liners were placed at the bottom of the deck panel formwork, and concrete was poured into the formwork. These deck panel specimens with engineered textures were cast in an upside-down position to facilitate the texture preparation. A standard broom, as is typically used in a precast plant, was borrowed from a plant in Omaha, Nebraska (Coreslab Structures), and the broom finish texture was created by pushing the broom over the top of the surface one time two hours after pouring the concrete. All specimens were constructed using concrete with a specified strength of 4 ksi, which is the normal Iowa DOT bridge deck mix. The formwork was removed 3 days after pouring, and the specimens were left to air cure for 28 days.

After curing consistent with Iowa DOT standards, a 1.25 in. thick overlay was placed on each deck panel specimen. This was accomplished by placing wet UHPC on the rough surface of the normal concrete. Commercially available standard Ductal mix produced by Lafarge North America was used as the UHPC overlay in this project. Prior to pouring the UHPC overlay, the normal concrete deck panels with textures were dampened to minimize the water loss from the UHPC mix due to absorption by the unsaturated normal concrete deck panel (see Figure 24).
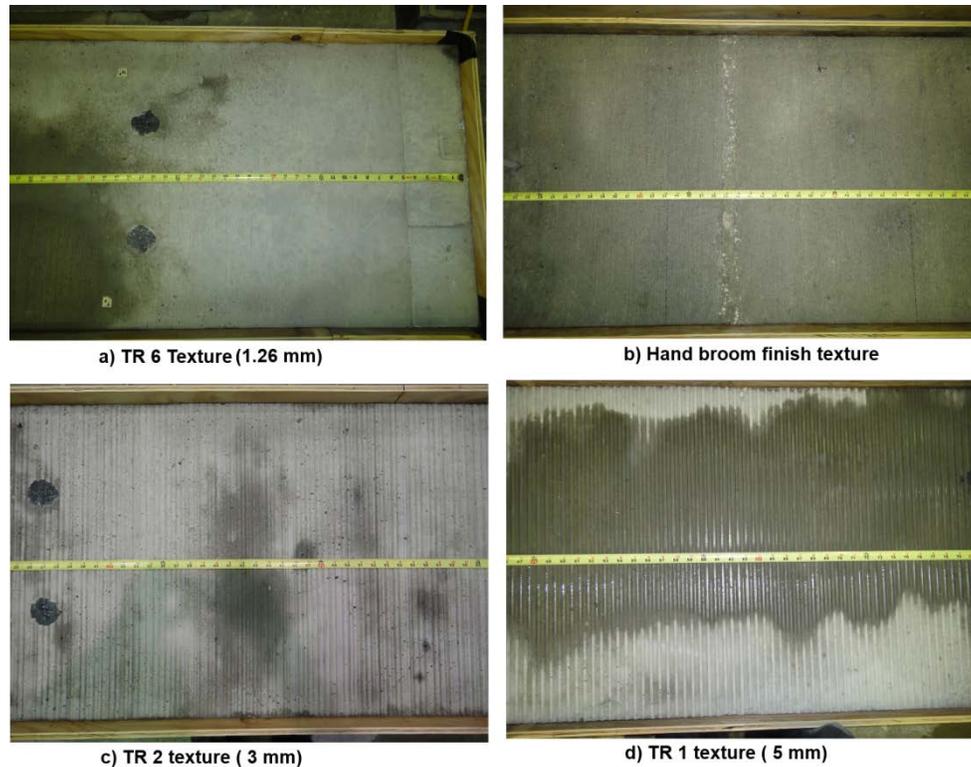
Figure 24. Normal concrete deck specimens with surface texture prior to pouring UHPC overlay

The UHPC was mixed in the laboratory using a Mortarman750 mixer and was placed immediately on the deck panel formwork. Standard compression test cylinders (3 in. × 6 in.) and modulus beams were cast for every pour to establish the strength gain of the panel with time. A standard flow table was used to measure the flowability of UHPC for the pour. The measured flow for the UHPC was more than the recommended value of 8 in., validating the quality of the overlay mix. After casting, the composite panels were covered with a plastic tarp to minimize water evaporation from the UHPC and were then air cured. All specimens were supported on 2 in. × 4 in. wood supports (commonly called 2 by 4s) set at a distance of 7 ft apart. No additional heat treatment was provided to accelerate the strength gain of the UHPC so that the specimen preparation would mimic field conditions for overlays as much as possible in the laboratory. The plastic tarp on the UHPC was removed after 2 days, and the specimens were air cured for 28 days. All of the cylinders were also air cured to mimic the specimen curing conditions. The measured compressive strengths of NC and UHPC at 28 days after casting were found to be 4.55 ksi and 15.5 ksi, respectively.

During the curing time period, 1 week after the UHPC pouring, delamination of the UHPC overlay was observed over a small section at the end of a composite specimen with the TR6 texture. The delamination was attributed to the high shrinkage of UHPC and the shallow texture depth of the interface. The length of the delamination grew over time and reached nearly 50% of the interface length at 28 days. No delamination was observed in any other specimens. This observation indicates that although the slant shear test may adequately characterize the interface behavior, it cannot capture the potential delamination associated with differential shrinkage. It

51

should be noted that slant shear test results do not account for the shrinkage effect on reducing the interface strength. Therefore, when using the slant shear test results for design purposes, one should use a higher safety factor when utilizing the bond strengths obtained from slant shear tests. Also, this observation suggests the need for a detailed study to understand UHPC shrinkage effects on interface and deck panel behavior, preferably a test conducted in the field. A repair was attempted on the delaminated specimen by injecting epoxy resin into the surface. It was learned that the epoxy injection using the standard Iowa DOT procedure helped to address the delamination issue. However, due to the delamination and the subsequent repair, the specimen was excluded from this study.

The standard overlay deck specimen was constructed using Iowa DOT standard procedure for concrete overlays. The normal deck concrete specimen was constructed with the same concrete mix as the other four UHPC-NC composite specimens. The surface of this specimen was finished with a trowel. After allowing the specimen to cure for 60 days, a very stiff overlay mix with a low water-cement ratio was prepared at the ISU structures laboratory according to Iowa DOT overlay specifications. A local bridge contractor helped with the placement of the overlay to mimic the field placement of standard overlays. Prior to placing the standard overlay, a thin cement paste slurry was smeared on the normal deck concrete specimen to improve the bonding between the deck and the overlay concrete. Wet burlap was placed on the composite specimen for three days to minimize water evaporation and shrinkage. After three days, the specimen was allowed to air cure. The measured concrete strength of the overlay mix at seven days was found to be 6.9 ksi.

3.3.2 Test Setup

The setup used for testing the UHPC-NC composite deck specimens is shown in Figure 25.
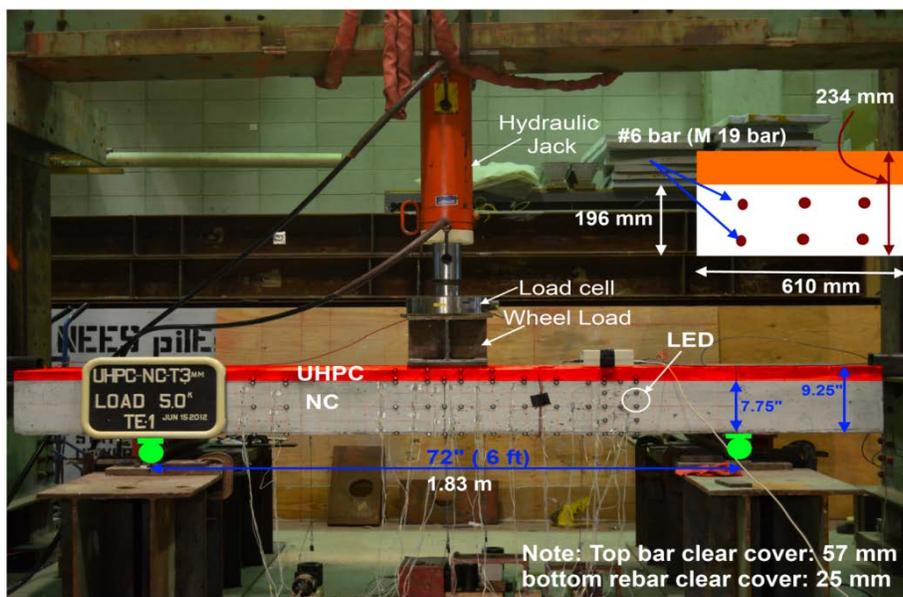

Figure 25. Test setup for the flexural testing of concrete deck specimens with UHPC overlay

The 8 ft long test specimens were simply supported on rollers with a 6 ft clear span. This simply supported test configuration was chosen to maximize the flexure and shear demand on the deck panel and, in turn, maximize the interface stresses at the UHPC-normal concrete interface. The load was applied at the center of the specimen with a hydraulic actuator and was measured using a 100 kip load cell. A 10 in. × 20 in. steel plate, representing a standard truck wheel contact area, in accordance with AASHTO LRFD guidelines for bridges, was used to distribute the load to the deck panel.

3.3.3 Loading

The performance of the UHPC-NC composite sections with different interface textures was evaluated using two different load regimes under two different wheel load orientations. This was done to introduce different flexural stresses at the interface along the middle of the span using the same shear force and to capture the strength degradation with repeated loading. The load orientations indicated the direction of wheel load width (i.e., 20 in.) with respect to the direction of the specimen's longitudinal axis. As shown in Figure 26(a) and 26(b), load orientations A and B represented the wheel loads, where the wheel width (20 in.) was along the longitudinal (traffic direction) and transverse directions, respectively.

a) Load Orientation-A   b) Load Orientation-B

Figure 26. Load orientations used in flexural testing of composite deck specimen

Load orientation A will subject the specimen to higher bending stresses for the same shear force compared to load orientation B.

The load regimes indicated the extent of damage for a given load orientation. All of the specimens were subjected to two load regimes for both load orientations. In Load Regime 1, the specimens were subjected to loads just above the calculated cracking values. In Load Regime 2, the specimens were subjected to loads designed to cause significant cracking and failure of the specimens in shear or interface debonding.

All specimens were load tested in the following order: (1) loading up to 12.5 kips in load orientation A, (2) loading and unloading up to 21.3 kips and 48 kips in load orientation B to represent the service load conditions expected on the prototype bridge, (3) loading up to 60 kips using load orientation A to cause shear cracking in the normal concrete, and (4) loading to failure

in load orientation B to estimate the capacity of the system. The details of the applied loading for different specimens are shown in Figure 27.
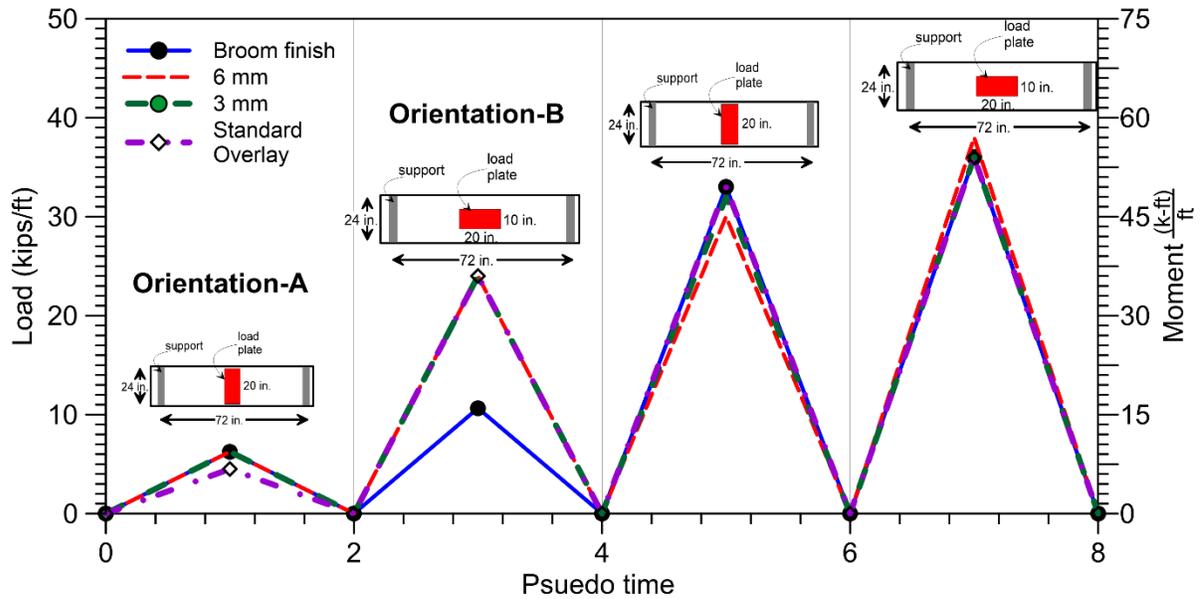

Figure 27. Load protocols used for testing of composite deck specimen

3.3.4 Instrumentation

This section presents the details of the instrumentation used to monitor the performance of the composite deck specimens during testing. Several different types of instruments were used for this study, including LVDTs, string potentiometers, and a state-of-the-art, three-dimensional (3D) Optotrak system. A total of five string potentiometers were used to measure vertical displacements along the span of the composite specimens. The string potentiometers were located at the quarter points (i.e., 18 in. from the supports), at the center (i.e., below the load), and at 5 in. from the center (i.e., at the edge of the load in Configuration A). The locations and identifications used for these string potentiometers are shown in Figure 28, with 28(a) showing the specimen with the TR texture, 28(b) showing the specimen with the TR1 texture, 28(c) showing the specimen with the broom-finish texture, and 28(d) showing the normal concrete specimen.

a) UHPC-NC Specimen with TR 2 texture (3mm)

b) UHPC-NC Specimen with TR1 Texture (5 mm)

c) UHPC-NC specimen with hand broom finish texture

d) NC-NC standard overlay specimen
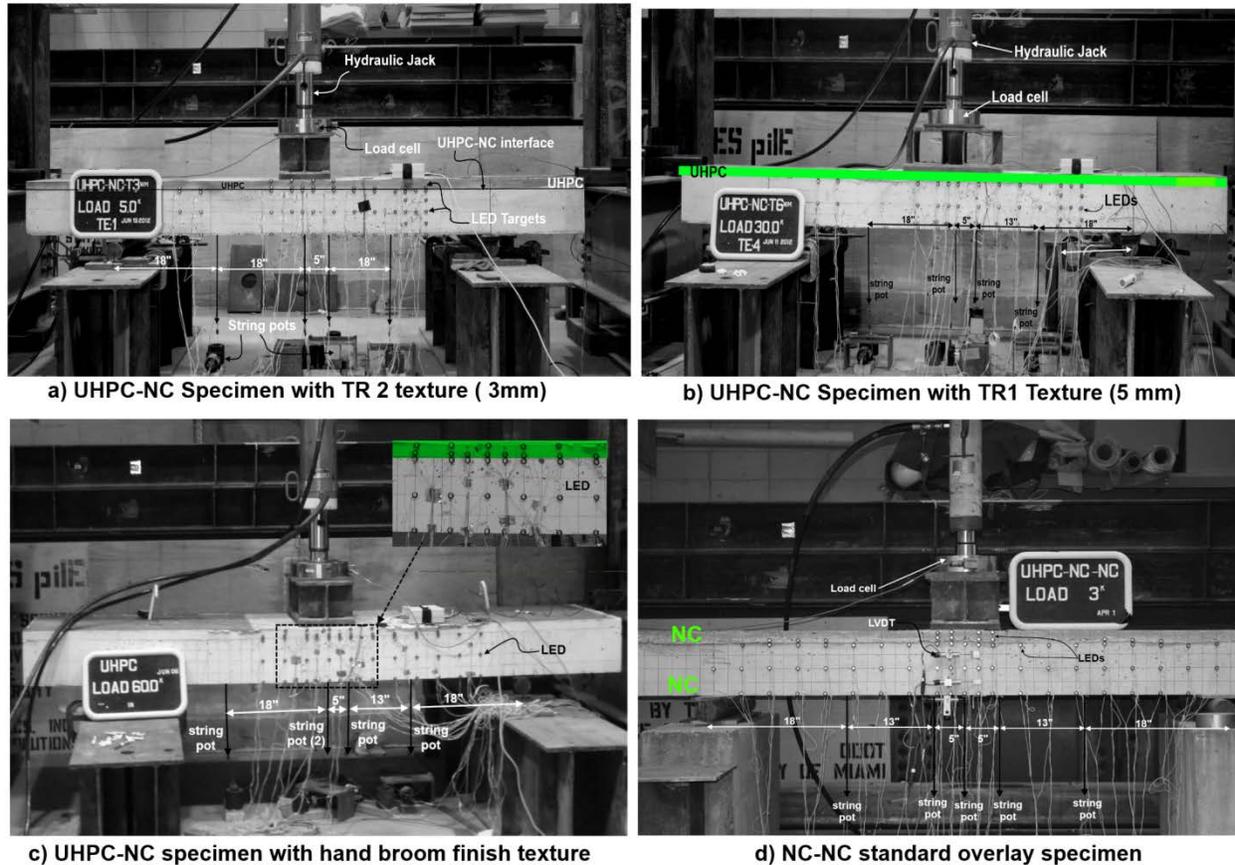
Figure 28. Instrumentation used to capture the slab and interface behavior

The Optotrak system consists of a state-of-the-art 3D camera and LED targets. 3D ordinates of the LED targets are captured by the camera at a frequency of 10 Hz using photogrammetry principles. Each specimen was instrumented with at least 54 LEDs to capture the vertical deformations, shear deformations, and slip between the UHPC layer and the NC layer as well as curvatures along the span and depth of the specimen. The LED targets were attached to the specimen using standard hot glue, as recommended by the manufacturer. The LED targets were hot glued on a 2 in. grid, as can be seen on the different specimens in Figure 28. During the test, the data from all gauges and displacement devices were recorded using a computer-based data acquisition system at a 1 Hz frequency.

3.3.5 Experimental Observations

At the service-level loading of 21.3 kips, a few hairline flexural cracks were observed in the normal concrete directly under the load in all of the specimens. All specimens ultimately failed with the initiation of shear failure in the normal concrete portion of the composite deck at a load in the range of 70 kips, which is nearly 4.4 times the designed service-level wheel load. The slip along the UHPC-NC interface was monitored using a state-of-the-art 3D Optotrak system with LED targets. No slip was observed at the interface until the initiation of shear failure in the

specimens. The measured force displacement responses of all four specimens are shown in Figure 29, and the eventual damaged states at failure are shown in Figure 30.
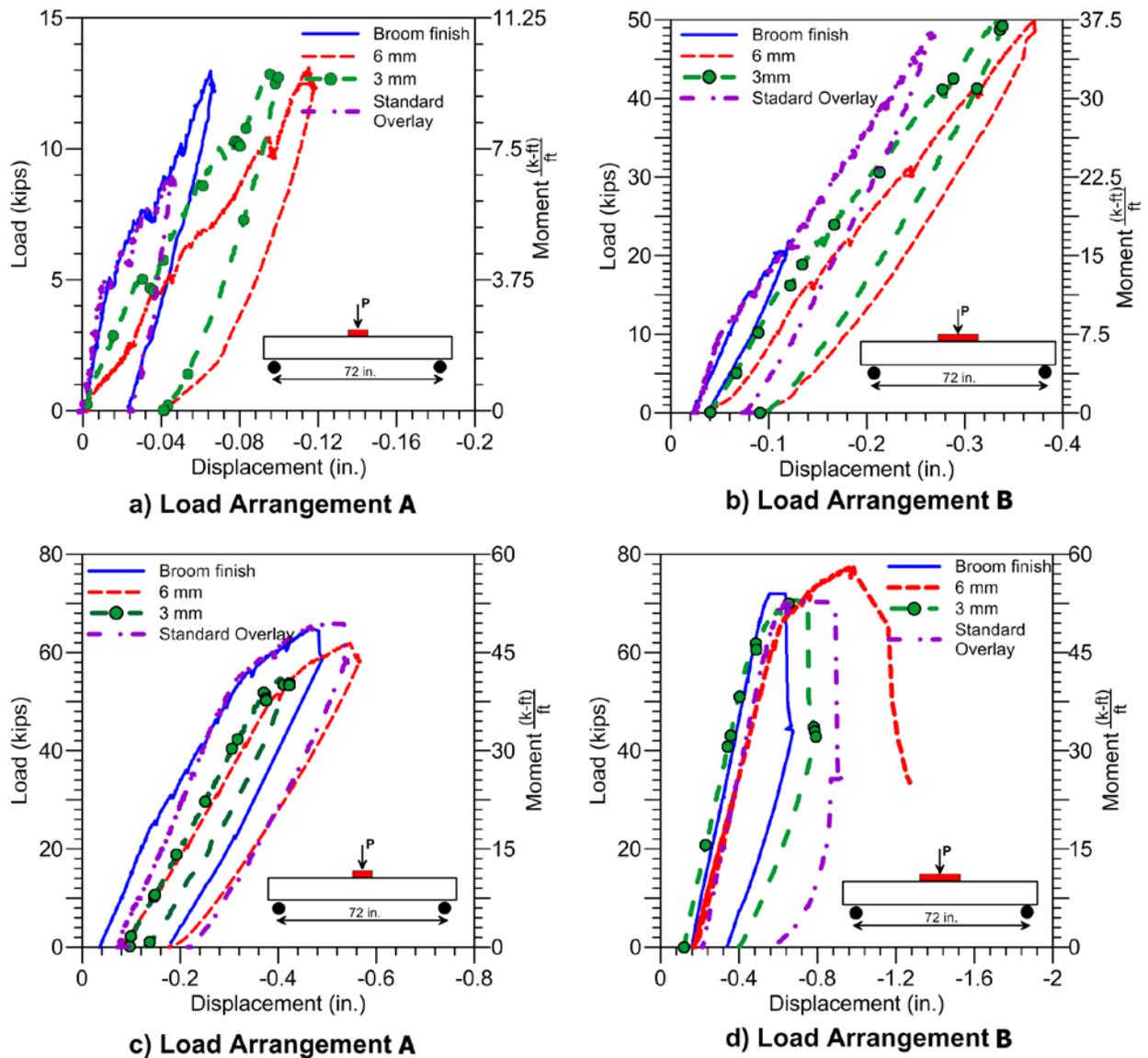

Figure 29. Measured force-displacement response of composite test specimens

a) UHPC-NC specimen with hand broom finish texture

b) UHPC-NC specimen with TR1 (5mm) Texture

c) UHPC-NC specimen with TR2 (3mm) texture

d) NC-NC standard overlay specimen
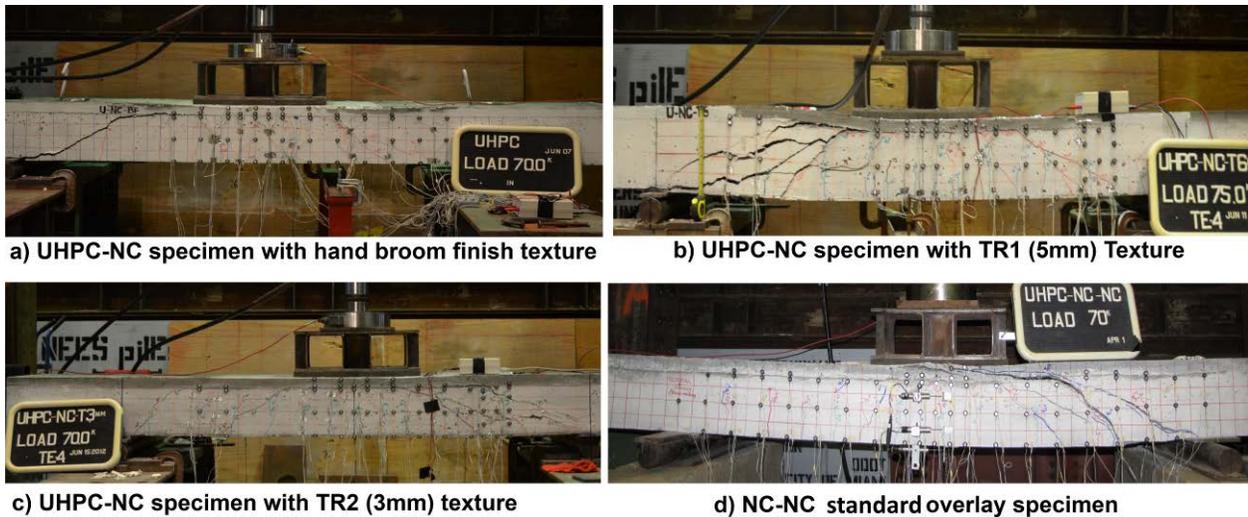
Figure 30. Cracking in the composite specimens at the ultimate failure load

From observing Figure 29, it is clear that all three interfaces would be adequate for composite action. However, the broom finish specimen did not experience any significant ductility compared to other two specimens.

Once the shear capacity of the composite deck was reached, delamination of the UHPC overlay was observed, which appeared to be triggered by the shear cracking in the normal concrete. The shear crack in the normal concrete did not penetrate through the UHPC overlay. Instead, the crack propagated horizontally along the interface, causing delamination. In the other two specimens, due to a higher interface capacity resulting from a deeper interface texture, the delamination due to shear cracking in the normal concrete did not occur until there was a greater amount of deformation compared to the broom finish specimen. The deeper interface texture also caused wider shear cracks in the specimens (see Figure 30 (b) and (c), leading to larger shear deformations, greater yielding of the reinforcement, and higher displacement capacity at failure.

3.3.5.1 Moment - Curvature Response:

The experimental curvature at the center of the composite beam was estimated using the LED deformations. The average strain at five different locations along the depth of the composite beams was estimated for each load at one-kip increments by dividing the deformation between a pair of adjacent LEDs by the corresponding initial length. The strain distributions in the three composite specimens along the height for a service load of 21.3 kips and an overload of 48 kips are show in Figure 31. A first order linear curve was fitted to the strain variation along the depth, and the slope of the best fit line provided the average curvature.
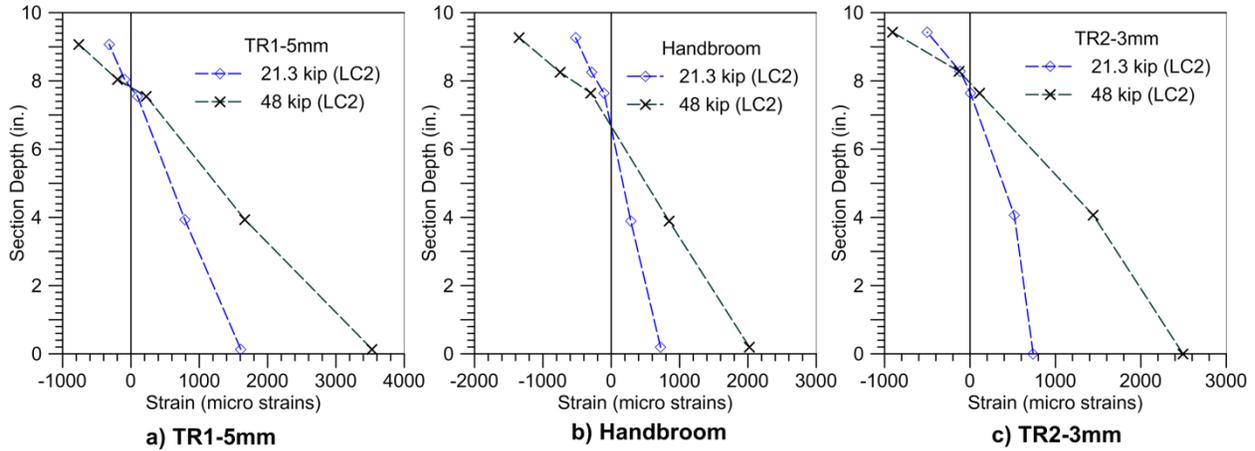
Figure 31. Strain distributions along the depth of the composite specimens

The measured moments vs. curvature responses for all the specimens are shown in Figure 32.
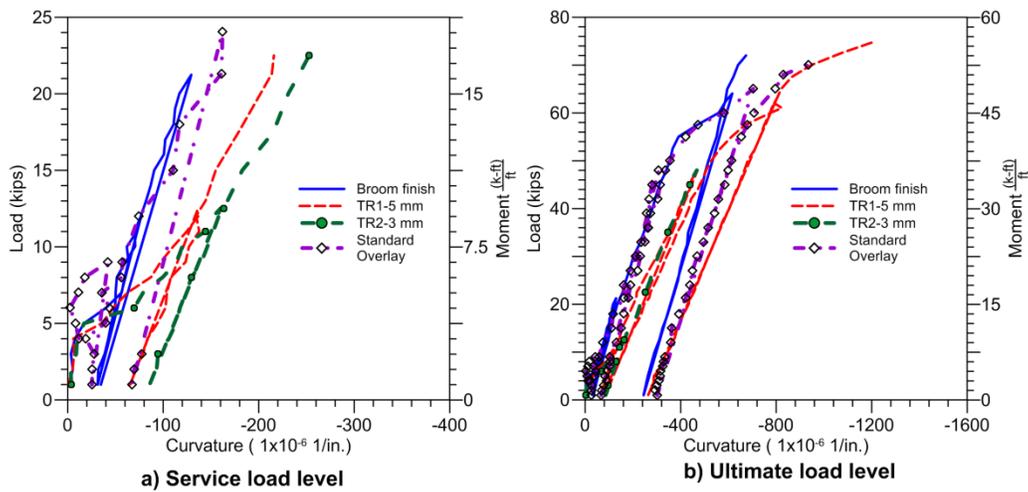
Figure 32. Measured moment-curvature response at mid-span for all composite specimens

3.3.5.2 Interface Shear demand (ACI 318-11)

ACI 318 (2011) allows designers to compute the horizontal shear stress at the interface of composite sections using two methods based on (1) the global force equilibrium conditions and (2) the simplified beam elastic theory. ACI 318-11 Sec. 17.5.4 allows designers to estimate the horizontal shear stresses at the interface of a composite section using global force equilibrium conditions. According to that section of the ACI specification, the change in compressive or tensile force in the slab (overlay) in any segment of its length is equal to the interface shear force. In other words, for a simply supported beam, as shown in Figure 33, the interface shear force between Sections A and B (see Figure 33) is given as

$$V_h = C_B - C_A \Rightarrow v_h = \frac{C_B - C_A}{b\,l}$$

(15)

where V_h = interface shear force over the distance l, v_h = horizontal shear stress at the interface, $C_B - C_A$ = change in the compressive force between sections A and B, b = width of the interface, and, l = length over which the horizontal shear is to be transferred.
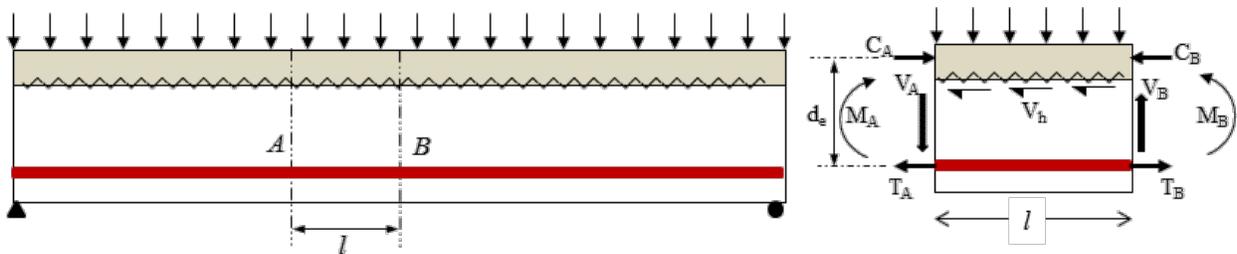

Figure 33. Shear stresses along the interface in a simply supported beam

Using the simplified elastic beam theory, the equation can be written as

$$V_h = C_B - C_A \Rightarrow v_h = \frac{\dfrac{M_B}{d_e} - \dfrac{M_A}{d_e}}{b\,l} = \frac{\dfrac{M_B}{l} - \dfrac{M_A}{l}}{b\,d_e} = \frac{V}{b d_e}$$

(16)

where V_h = horizontal shear stress, V = factored vertical shear force at a section we estimate the horizontal shear stress, and d_e = the distance from the extreme compression force for the entire composite section to the centroid of the prestressed and non-prestressed longitudinal tension reinforcement.

ACI 318-11 (Section 17.5.2) recommends that this value need not be taken as less than 0.80 h for prestressed concrete members, where h is the height of the composite section. Section 5.8.4.2 of AASTHO (2010) recommends that d_e be taken as the distance between the centroid of the tension steel to the mid-thickness of the overlay.

Because none of the composite specimens experienced any slippage along the interface up to the shear failure of the specimen, the interface shear stress for different interfaces can be estimated using the above equation. The minimum interface shear capacity of the standard overlay, hand broom texture, TR2-3mm interface, and the TR1-5mm interfaces were 186 psi, 195 psi, 190 psi, and 215 psi, respectively. These numbers are much lower than the bond capacity estimated using the slant shear tests. In comparison to these interface shear capacities, the slant shear test produced 15 to 25 times more resistance. This implies that if the shear failure in the normal concrete of the beam had not initiated, the beam with the UHPC overlay could have resisted much higher loads.

3.3.6 Analytical Modeling

Based on the experimental observations, there was no delamination observed at the interface between the UHPC and the normal concrete. The structural response of the composite UHPC-NC members was estimated by extending the commonly used flexural design model for reinforced concrete and considering the compression and tensile behavior of UHPC. The analytical model for bending is based on the following hypotheses:

- Plane sections remain plane, indicating that the strain profile along the depth of the section is linear. This means that a perfect bond is assumed between the normal concrete and the UHPC at the interface (i.e., no debonding occurs at the interface, and the structural element shows monolithic behavior).

- There is a perfect bond between the cementitious materials (concrete and UHPC) and steel reinforcement.

- The behaviors of steel, UHPC, and concrete materials are known and described with standard material laws.

- The cross-section is in equilibrium; i.e., the equilibrium of forces and moment is maintained at the section level.

The compressive stress-strain behavior of UHPC was established in numerous concrete compressive cylinder tests and is presented in Chapter 2. Unlike normal concrete, the measured stress-strain relationship for UHPC was found to be linear up to 80 to 90% of the peak stress under both heat curing and air curing conditions. Also, the maximum measured compressive strains in the UHPC layer of the composite specimen were below 2000 micro strains (see Figure 31). Hence, the UHPC compression stress-strain behavior is modeled with a linear elastic curve with a modulus of elasticity of 7500 ksi.

The tensile strength and post-cracking behavior of UHPC depends on the strength, quantity (e.g., volume by percentage), length, and orientation of the steel fibers, which effectively prevent or delay the opening of concentrated cracks. The tensile strength is also influenced by the type of curing condition (steam vs. air cured) provided for the UHPC members. The tensile stress-strain calculations were taken from a set of direct tension tests conducted on large steam-cured dog-bone specimens (Sritharan et al. 2003). The tensile stress-strain behavior established in these dog-bone tests, which have been used successfully in characterizing the flexural response of UHPC full-scale bridge girders, tapered H-shaped piles, and waffle deck panels, is utilized in this analytical model. However, for the UHPC-NC composite specimen tested in this study, the UHPC overlay is predominantly in compression, except at loads beyond 48 kips. At that point, the UHPC near the interface was in tension. However, the corresponding tensile strains were below 200 micro strains (see Figure 31). In this range, the tensile behavior can be represented with a linear curve. The stress-strain behavior of steel is represented using an elastic-perfectly

plastic curve with a measured yield stress of 71.8 ksi. The typical strain and stress distribution along the section depth are shown in Figure 34.
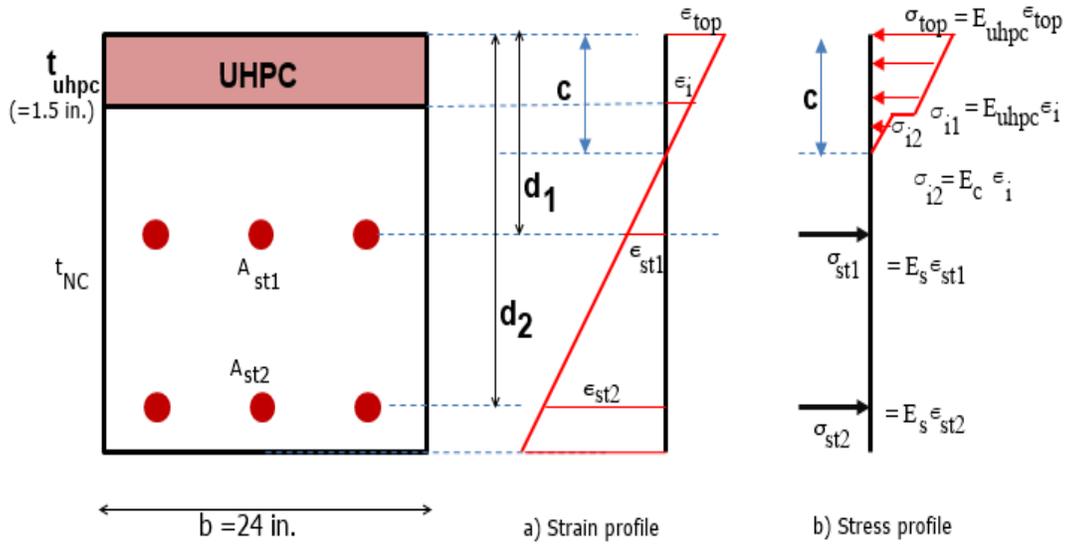
Figure 34. Analytical model used for the composite specimen

Using the equilibrium conditions, the neutral axis depth, c, can be calculated for an assumed strain at the top surface, ε_{top}. The moment capacity of the section is estimated by taking the moment of all forces (compression in both the UHPC and normal concrete and tension in reinforcement) at the top of the beam. The comparison between the experimental moment-curvature responses and the calculated response is shown in Figure 35.
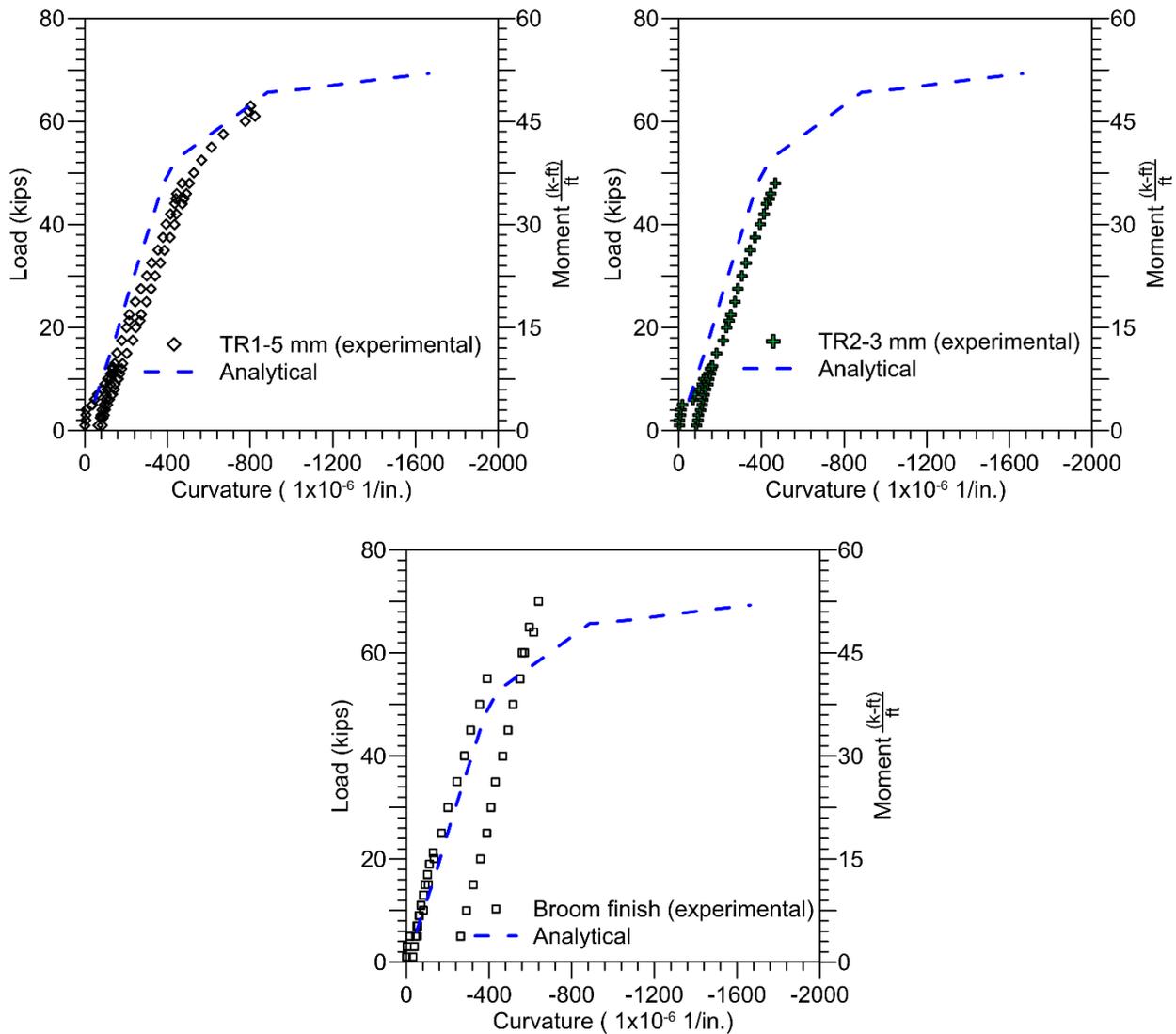
Figure 35. Comparison of experimental and analytical moment curvature response

The calculated moment-curvature response was within 10% of the measured values for all the test specimens. The stiffness of all the specimens from testing was slightly lower than the value predicted by the analytical model. This is to be expected, because the simplified analytical model does not account for any formation of localized cracks. The maximum load capacity calculated using the analytical model is 69.3 kips. This value is within 3% of the experimentally measured capacities of the 3 mm and broom finish texture specimens and 10% of the 6 mm texture specimens, respectively. So, one can use these simplified analytical models to estimate the capacities of the UHPC-NC specimens.

4 SUMMARY AND CONCLUSIONS

4.1 Summary

UHPC is a relatively new class of high strength concrete material with self-leveling characteristics in addition to excellent durability and tensile strength properties when compared to NC used in today's bridge construction. Previous experimental research on material characterization has shown that UHPC has negligible chloride ion permeability, very high freeze-thaw resistance, no alkali silica reaction, and no scaling, even with an ambient air curing regime. Consequently, UHPC has gained significant momentum in terms of its utilization in bridge applications among several DOTs and the FHWA. Its unique combination of excellent strength, exceptional durability, and flexible constructability also makes UHPC an ideal material for minimizing deck cracking, especially as an overlay for concrete bridge decks or as a protective layer for new bridge decks. These uses would allow a designer to minimize the cost of a UHPC deck system while overcoming the deck deterioration that frequently occurs due to surface cracking and the subsequent penetration of deicing chemicals applied to the top surface.

The performance of a UHPC-NC composite system depends largely on how well the UHPC is used as an overlay material, how tightly it bonds to the normal concrete substrate, and how durable the overlay material is. This research project explored the use of UHPC as an overlay for concrete bridge decks and evaluated the influence of several parameters on the success of such a use for UHPC, such as the normal concrete strength, the interface roughness, and the effect of the curing condition on the interface shear friction and bond behavior. The scope of the work presented herein is limited to an assessment of the bond strength between the UHPC and the normal concrete substrate. An integrated experimental and analytical study consisting of the slant-shear testing of UHPC-NC composite specimens and three-point bending of UHPC-NC deck slabs was conducted at ISU.

Slant Shear Testing: A total of 60 slant UHPC and NC interface specimens were tested to failure. This testing was performed to identify the most suitable interface for the UHPC-NC composite deck giving due consideration to constructability and interface strength, along with estimating the bond strength between the UHPC and the NC for different interface textures under variable curing conditions. The composite test specimens had five different texture depths ranging from 1.25 mm to 6 mm and were made from three different normal concrete strengths ranging from 5 ksi to 7.5 ksi. The testing examined the feasibility and effects of different interface textures, concrete strengths, and casting sequences on the shear friction behavior of the composite deck interface.

Flexural Testing: Following the investigation of bond behavior using the slant shear tests on the composite test units, a total of five specimens, including four UHPC-NC composite deck specimens with interface texture depths varying from 1.5 mm to 5 mm and one specimen with a standard concrete overlay, were tested under combined flexural and shear loading. All the specimens were tested to failure using a three-point bending configuration with a wheel load applied at the center of the composite deck specimen. All specimens ultimately failed with the initiation of shear failure in the normal concrete portion of the composite deck at a load of about

4.5 to 4.9 times the designed service-level wheel load. A simplified analytical model to explain the results was to estimate the strength of the composite deck specimen using traditional beam bending theory.

4.2   Conclusions

Based on the observations during specimen fabrication, experimental testing, and analytical modeling, the following conclusions have been drawn:

- For the slant shear test, the bond strength at the interface was highly dependent on interface roughness. The specimens with no surface roughness failed at the interface. The specimens with grooves or shear keys did not fail at the interface; instead, the normal concrete experienced splitting failure. These results indicate that proper surface preparation with sufficient roughness yields greater bond strength in shear/compression than the individual substrate material capacity.

- A minimum roughness of 2 mm was sufficient to develop adequate bond strength at the UHPC and NC interface under combined shear and compression loading. The casting sequence did not have any significant influence on the bond strength at the interface.

- Regardless of concrete strength, the UHPC-NC bond capacity at 28 days surpassed the requirements of ACI 546.3R-06 for all textures with texture depths greater than 2 mm. However, the average bond strength values with texture depths of less than 1.6 mm were below the recommended values for 5 ksi normal strength concrete mix. Therefore, if UHPC is applied to normal concrete with a surface roughness of 1.6 mm or less, delamination of the UHPC layer can occur.

- The analytical equations available in the literature, including the AASHTO (2010) equation for interface shear capacity, were found to be conservative in estimating the interface shear strength of UHPC and NC. However, the equation proposed by Santos and Júlio (2009) correlated well with the experimental values. The AASHTO (2010) equation provided the next best correlation with the experimental values. Hence, for design purposes, the use of the current AASHTO (2010) recommendations to estimate the interface shear capacity is appropriate.

- Delamination of the UHPC overlay was observed in a specimen with an interface texture of only 1.25 mm. This indicates that the volume changes in UHPC due to shrinkage and the restraint from the underlying old concrete deck led to internal stresses greater than the interface bond strength at that depth.

- Flexural testing of the composite UHPC-NC deck specimens yielded no interface failures. There was no interfacial slip during testing. Experimental results demonstrated that the maximum shear stresses at the interface ranged from 150 to 200 psi at the deck shear failure load, which are much lower than the bond strengths observed in the slant shear tests.

- Based on the flexural tests on composite slabs, it is clear that UHPC can be used as a durable overlay in bridge decks. Given that the investigation focused largely on short-term effects, 3 mm minimum roughness is recommended for the UHPC and NC interface.

- The behavior of the UHPC-NC composite section can be accurately calculated using analytical models based on traditional beam bending theory with appropriate material stress-strain characteristics.

4.3 Future Research

The following topics need to be addressed through future research before implementing UHPC-NC composite decks or UHPC overlays in routine field applications:

- The differential volume change of the overlay induces stresses along the interface and in the concrete substrate materials. During this project, delamination was observed in a composite specimen under air-cured conditions. Further research on large-scale specimens is needed to understand the effects of thermal variations, differential shrinkage, and creep on the long-term performance of composite decks.

- The integrity of the UHPC bridge deck overlay should be evaluated under high cyclic fatigue loading.

- There is very limited research available in the literature that addresses the effects of freeze-thaw cycles and deicing salt on the interface bond behavior. Further research needs to be conducted on large-scale samples to understand the long-term performance and cost effectiveness of a UHPC overlay.

- In the current study, the UHPC overlay and the interface were predominantly in compression, representing the state of stress on a simple span bridge. However, on a continuous span bridge, the stress at the interface and the UHPC at locations of maximum negative bending will be different. Therefore, experimental and analytical studies involving multi-span bridges should be conducted.

- Existing cracks in concrete bridge decks may create localized stresses, which may lead to cracking or debonding of the UHPC overlay. The effect of these localized stresses and the possibility of crack propagation through the depth of the UHPC overlay should be investigated.

REFERENCES

Aaleti, S., B. Peterson, and S. Sritharan. 2013. *Design Guide for Precast UHPC Waffle Deck Panel System, Including Connections*. Federal Highway Administration, Washington, DC.

Aaleti, S., S. Sritharan, D. Bierwagen, and T. Wipf. 2011. Structural Behavior of Waffle Bridge Deck Panels and Connections of Precast Ultra-High-Performance Concrete: Experimental Evaluation. *Transportation Research Record: Journal of the Transportation Research Board,* No. 2251, pp. 82–92.

AASHTO. 2010. *AASHTO LRFD Bridge Design Specifications*. 5th Edition, American Association of State Highway and Transportation Officials, Washington, DC.

ACI Committee 318. 2011. *Building Code Requirements for Structural Concrete (ACI 318–11) and Commentary*. American Concrete Institute, Farmington Hills, MI.

ACI Committee 546. 2004. *Concrete Repair Guide.* American Concrete Institute, Farmington Hills, MI.

Ahlborn, M. T., J. E. Peuse, and L. D. Misson. 2008. *Ultra-High-Performance-Concrete for Michigan Bridges Material Performance – Phase I.* Michigan Tech Center for Structural Durability, Michigan Tech Transportation Institute, Houghton, MI.

Badoux, J. C. and C. L. Hulsbos. 1967. Horizontal Shear Connection in Composite Concrete Beams under Repeated Loads. *Journal of the American Concrete Institute*, Vol. 64, No. 12, pp. 811–19.

Banta, T. E. 2005. Horizontal Shear Transfer between Ultra High Performance Concrete and Lightweight Concrete. MS thesis. Virginia Polytechnic Institute and State University, Blacksburg, VA.

Bergren, J. V. and B. C. Brown. 1975. *An Evaluation of Concrete Bridge Deck Resurfacing in Iowa: Special Report*. Iowa State Highway Commission, Ames, IA.

Bierwagen, D. and A. Abu-Hawash. 2005. Ultra High Performance Concrete Highway Bridge. *Proceedings of the 2005 Mid-Continent Transportation Research Symposium*, Ames, IA, August 18–19, pp. 1–14.

Birkeland, P. W. and H. W. Birkeland. 1966. Connections in Precast Concrete Construction. *Journal of the American Concrete Institute*, Vol. 63, No. 3, pp. 345–68.

Carbonell Muñoz, M. A. 2010. Compatibility of Ultra High Performance Concrete as Repair Material: Bond Characterization with Concrete under Different Loading Scenarios. MS thesis. Michigan Technological University, Houghton, MI.

Crane, K. C. 2010. Shear and Shear Friction of Ultra-High Performance Concrete Bridge Girders. PhD dissertation. Georgia Institute of Technology, Atlanta, GA.

Denarié, E. 2005. Full Scale Application of UHPFRC for the Rehabilitation of Bridges – from the Lab to the Field. European Project 5th European Frameworks Programs, Deliverable D32, Sustainable and Advanced MAterials for Road Infrastructure (SAMARIS).

Garcia, H. and B. Graybeal. 2007. *Analysis of an Ultra-High Performance Concrete Two-Way Ribbed Bridge Deck Slab*. Tech Brief No. FHWA-HRT-07-055. Federal Highway Administration, Turner-Fairbank Highway Research Center, McLean, VA. https://www.fhwa.dot.gov/publications/research/infrastructure/bridge/07055/07055.pdf

Graybeal, B. A. 2006. *Material Property Characterization of Ultra-High Performance Concrete.* Report No. FHWA-HRT-06-103. Federal Highway Administration, Turner-Fairbank Highway Research Center, McLean, VA. https://www.fhwa.dot.gov/publications/research/infrastructure/structures/06103/06103.pdf

Graybeal, B. 2012. *Ultra-High Performance Concrete Composite Connections for Precast Concrete Bridge Decks.* Tech Brief No. FHWA-HRT-12-042. Federal Highway Administration, Turner-Fairbank Highway Research Center, McLean, VA. https://www.fhwa.dot.gov/publications/research/infrastructure/structures/hpc/12042/12042.pdf

Hanson, N. W. 1960. Precast-Prestressed Concrete Bridges: Horizontal Shear Connections. *Development Department Bulletin D35*, Portland Cement Association, Vol. 2, No. 2, pp. 38–58.

Keierleber, B., D. Bierwagen, T. Wipf, and A. Abu-Hawash. 2008. Design of Buchanan County, Iowa Bridge Using Ultra-High Performance Concrete and Pi-Girder Cross Section. *Proceedings of the Precast/Prestressed Concrete Institute National Bridge Conference*, Orlando, FL, October 4–7.

Kepler, J. L., D. Darwin, and C. E. Locke, Jr. *Evaluation of Corrosion Protection Methods for Reinforced Concrete Highway Structures.* University of Kansas Center for Research, Inc., Lawrence, KA.

Kollmorgen, G. A. 2004. Impact of Age and Size on the Mechanical Behavior of an Ultra-High Performance Concrete. MS thesis. Michigan Technological University, Houghton, Michigan.

Krauss, P. D., S. J. Lawler, and A. K. Steiner. 2009. *Guidelines for Selection of Bridge Deck Overlays, Sealers, and Treatments*. National Transportation Research Board, National Academy Press, Washington, DC.

Mansur, M. A., T. Vinayagam, and K. H. Tan. 2008. Shear Transfer Across a Crack in Reinforced High-Strength Concrete. *Journal of Materials in Civil Engineering,* Vol. 20, No. 4, pp. 294–302.

Mattock, A. H. 1988. Reader Comments. *Journal of the Precast/Prestressed Concrete Institute,* Vol. 33, No. 1, pp.165–6.

Mattock, A. H. 1981. Cyclic Shear Transfer and Type of Interface. *ASCE Journal of Structural Engineering,* Vol. 107, No. 10, pp. 145–64.

Mattock, A. H. and N. M. Hawkins. 1972. Shear Transfer in Reinforced Concrete – Recent Research. *Journal of the Precast/Prestressed Concrete Institute,* Vol. 17, No. 2, pp. 55–75.

Mattock, A. H., W. K. Li, and T. C. 1976. Shear Transfer in Lightweight Reinforced Concrete. *Journal of the Precast/Prestressed Concrete Institute*, Vol. 21, No. 1, pp. 20–39.

Mau S. and T. Hsu. 1988. Reader Comments. *Journal of the Precast/Prestressed Concrete Institute,* Vol. 33, No. 1, pp.165–8.

Papanicolaou, C. G. and T. C. Triantafillou. 2002. Shear Transfer Capacity Along Pumice Aggregate Concrete and High-Performance Concrete Interfaces. *Materials and Structures*, Vol. 35, No. 4, pp. 237–45.

Perry, V. and D. Zakariasen. 2004. First Use of Ultra-High Performance Concrete for an Innovative Train Station Canopy. *Concrete Technology Today*, Vol. 25, No. 2, pp. 1–2.

Randl, N. 1997. Investigations on Transfer of Forces between Old and New Concrete at Different Joint Roughness. PhD dissertation. University of Innsbruck, Innsbruck, Austria.

Rouse, J. M., T. J. Wipf, B. Phares, F. Fanous, and O. Berg. 2011. *Design, Construction, and Field Testing of an Ultra High Performance Concrete Pi-Girder Bridge*. Bridge Engineering Center, Iowa State University, Ames, IA.

Russell, H. G. 2004. *NCHRP Synthesis 333: Concrete Bridge Deck Performance*. National Cooperative Highway Research Program, Washington, DC.

Saemann, J. C. and G. W. Washa. 1964. Horizontal Shear Connections between Precast Beams and Cast-In-Place Slabs. *Journal of the American Concrete Institute*, Vol. 61, No. 11, pp. 1309–83.

Santos, P. M. D., and E. N. B. S. Júlio. 2010. Effect of Filtering on Texture Assessment of Concrete Surfaces. *ACI Materials Journal*, Vol. 107, No. 1, pp. 31-36.

Santos, P. M. D. 2009. Assessment of the Shear Strength between Concrete Layers. PhD dissertation. University of Coimbra, Coimbra, Portugal.

Sarkar, J. 2010. Characterization of the Bond Strength between Ultra High Performance Concrete Bridge Deck Overlays and Concrete Substrates. MS thesis. Michigan Technological University, Houghton, MI.

Schmidt, M. and E. Fehling. 2005. Ultra-High-Performance Concrete: Research, Development and Application in Europe. *7th International Symposium on Utilization of High Strength High Performance Concrete*, Vol. 1, pp. 51–77.

Sritharan, S. 2015. Design of UHPC Structural Members: Lessons Learned and ASTM Test Requirements. *Advances in Civil Engineering Materials*, Vol. 4, No. 2, pp. 113–131.

Sritharan, S., B. Bristow, and V. Perry. 2003. Characterizing an Ultra-High Performance Material for Bridge Applications under Extreme Loads. *Proceedings of the 3rd International Symposium on High Performance Concrete*, Orlando, Florida.

Stantill-McMcillan, K. and C. A. Hatfield. 1994. Performance of Steel, Concrete, Prestressed Concrete, and Timber Bridges. In *Developments in Short and Medium Span Bridge Engineering '94: Proceedings of 4th International Conference on Short and Medium Span Bridges*, Halifax, Nova Scotia, Canada, August 8–11. The Canadian Society for Civil Engineering, Canada, pp. 341–354. www.woodcenter.org/docs/stanf94a.pdf.

Steele, G. W. and J. M. Judy. 1977. Polymer-Modified Concretes in Bridge Deck Overlay Systems. *Chloride Corrosion of Steel in Concrete*, pp. 110–115.

Transportation For America. 2013. *2013 Bridge Conditions.* www.t4america.org/resources/bridges/. Last accessed February 2013.

Vande Voort, T. L., M. T. Suleiman, and S. Sritharan. 2008. *Design and Performance Verification of UHPC Piles for Deep Foundations*. Center for Transportation Research and Education, Iowa State University, Ames, IA.

Walraven J., J. Frénay and A. Pruijssers. 1987. Influence of Concrete Strength and Load History on the Shear Friction Capacity of Concrete Members. *Precast/Prestressed Concrete Institute Journal*, Vol. 32, No. 1, pp. 66–84.

Walraven, J.C. 1981. Fundamental Analysis of Aggregate Interlock. *ASCE Journal of the Structural Division*, Vol. 107, No. 11, pp. 2245–70.

Wipf, T. J., B. M. Phares, S. Sritharan, E. B. Degen, and T. M. Giesmann. 2009. *Design and Evaluation of a Single-Span Bridge Using Ultra-High Performance Concrete*. Bridge Engineering Center, Iowa State University, Ames, IA.

ZellComp, Inc. 2011. *Infrastructure in Crisis*. www.zellcomp.com/infrastructure_crisis.html. Last Accessed on July 4, 2014.

Zilch, K. and R. Reinecke. 2000. Capacity of Shear Joints between High-Strength Precast Elements and Normal-Strength Cast-in-Place Decks. *PCI/FHWA/FIB International Symposium on High Performance Concrete*, Orlando, FL, September 25–27.